Multi-modal gait: A wearable, algorithm and data fusion approach for clinical and free-living assessment

Y Celik[1], S Stuart[2,3], WL Woo[1], E Sejdic[4,5,6,7], A Godfrey[1*]

[1] Department of Computer and Information Sciences, Northumbria University, Newcastle upon Tyne, NE1 8ST, UK
[2] Department of Sport, Exercise and Rehabilitation, Northumbria University, Newcastle upon Tyne, NE1 8ST, UK
[3] Northumbria Healthcare NHS foundation trust, North Tyneside General Hospital, Rake Lane, North Shields, Tyne and Wear, NE29 8NH
[4]Department of Electrical and Computer Engineering, Swanson School of Engineering. [5]Department of Bioengineering, Swanson School of Engineering. [6]Department of Biomedical Informatics, School of Medicine. [7]Intelligent Systems Program, School of Computing and Information. University of Pittsburgh, Pittsburgh, PA 15261, USA

***Corresponding author**
Alan Godfrey, PhD
Department of Computer and Information Sciences
Northumbria University
Newcastle upon Tyne
UK
NE1 8ST

Email: alan.godfey@northumbria.ac.uk

Abstract (300 words)
Gait abnormalities are typically derived from neurological conditions or orthopaedic problems and can cause severe consequences such as limited mobility and falls. Gait analysis plays a crucial role in monitoring gait abnormalities and discovering underlying deficits can help develop rehabilitation programs. Contemporary gait analysis requires a multi-modal gait analysis approach where spatio-temporal, kinematic and muscle activation gait characteristics are investigated. Additionally, protocols for gait analysis are going beyond labs/clinics to provide more habitual insights, uncovering underlying reasons for limited mobility and falls during daily activities. Wearables are the most prominent technology that are reliable and allow multi-modal gait analysis beyond the labs/clinics for extended periods. There are established wearable-based algorithms for extracting informative gait characteristics and interpretation. This paper proposes a multi-layer fusion framework with sensor, data and gait characteristics. The wearable sensors consist of four units (inertial and electromyography, EMG) attached to both legs (shanks and thighs) and surface electrodes placed on four muscle groups. Inertial and EMG data are interpreted by numerous validated algorithms to extract gait characteristics in different environments. This paper also includes a pilot study to test the proposed fusion approach in a small cohort of stroke survivors. Experimental results in various terrains show healthy participants experienced the highest pace and variability along with slightly increased knee flexion angles (≈1°) and decreased overall muscle activation level during outdoor walking compared to indoor, incline walking activities. Stroke survivors experienced slightly increased pace, asymmetry, and knee flexion angles (≈4°) during outdoor walking compared to indoor. A multi-modal approach through a sensor, data and gait characteristic fusion presents a more holistic gait assessment process to identify changes in different testing environments. The utilisation of the fusion approach presented here warrants further investigation in those with neurological conditions, which could significantly contribute to the current understanding of impaired gait.

Keywords; Wearable sensors, sensor fusion, gait analysis, multi-modal fusion, free-living

1. Introduction

Gait is a cyclic pattern of body movement, which advances an individual's position to perform daily life routines to maintain wellbeing [1]. Neurodegenerative diseases (e.g., stroke) can cause severe disruption to gait. Post-stroke, 50% of stroke survivors (SS) are unable to walk [2], and for those who can, asymmetrical gait is highly likely to occur with a large variance in different gait characteristics [3]. World health organisation (WHO) and Global Burden of Disease studies report falls are one of the leading causes of accidental deaths and injuries globally [4]. This can be due but not limited to lack of foot clearance in SS or freezing of gait (FoG) in Parkinson's disease when in the wild i.e., habitual ambulation/mobility during free-living in the home or community [5-7]. Therefore, regaining habitual ambulation has been identified as a major rehabilitation goal from early to late-stage in clinics and rehabilitation centres where the process of gait/walking assessment is usually performed to increase mobility and minimise fall risk [8].

Wearable technologies such as inertial measurement units (IMUs, which sense angular velocity and acceleration) can provide pragmatic gait data in the lab/clinic or beyond in the home and community (i.e. free-living) for more habitual assessments [9, 10]. As each anatomical segment of the human body has a characteristic movement pattern, wearable sensor location, calibration and methodologies must be carefully chosen considering the type of activity. The most preferred IMU-based wearable locations for gait analysis are waist, thighs, shanks, and feet [11] and have been used for a variety of different purposes such as activity detection [12], objective assessment of mobility, dynamic balance and concussion assessment [10, 13, 14], Parkinsonism and FoG [15] and phase detection of different neurological conditions [16, 17]. Typically, the current state of the art focuses on wearable IMU's for gait quality assessment. To date, studies have extracted different characteristics such as initial contact (IC) and final contact (FC) moments within the gait cycle to derive temporal parameters (e.g., step time) in various environments [18-21]. Additionally, spatial parameters (e.g. step length) are derived through additional modelling of inertial data [22, 23]. Those technical developments have enabled novel clinical studies to examine neurological gait in greater detail within a laboratory and free-living environments [24-28]. However, studies remain limited to a uni-modal (single IMU) approach and over reliance on temporal and spatial data only [29, 30].

Few studies have investigated multi-modal gait assessment and those that have are confined to indoor use [31-34]. Studies implementing multi-modal gait have utilised multiple IMU wearable and data fusion only for gait or physical activity detection [35-37]. The rationale for multiple (i.e. two or more) sensors attachment to e.g., shank and thigh includes: (1) provision of more reliable ground contact characteristics (IC and FC of the foot/feet) within the gait cycle as they are closer to the walking surface compared to waist and (2) enables additional gait capture, e.g. joint kinematics [38] such as knee flexion angles [39-42]. Yet, modern wearables go beyond IMU technologies by offering additional sensing modalities such as electromyography (EMG) within a single device. That is important as muscle activity (of the lower extremities) during gait needs to be well-coordinated to provide support, dynamic balance, propulsion, and foot clearance as examined during walking and stair ambulation [43, 44]. Thus, a more comprehensive gait assessment tool that utilises spatio-temporal characteristics (e.g., step time and step length), kinematic (e.g., joint angles) and muscle activation (e.g., muscle bursts) can and needs to be developed. The provision of a multi-modal (wearable/sensor, data, and gait characteristic) fusion approach could contribute to a more rounded understanding of impaired gait by providing quantitative spatio-temporal, kinetic and muscle characteristics of individuals. The developed multi-modal tool can enable clinicians to better measure the effectiveness of applied rehabilitation programs and track disease progression and its effects on gait especially for those with a neurological condition.

1.1 Fusion fit for the wild

Fusion of multiple measurement resources presents a promising development for human movement studies such as increased activity recognition and more informed gait assessment [45, 46]. Previously, IMU sensor fusion with accelerometers and gyroscopes was adopted to produce more consistent and reliable outputs [47]. Typically, accelerometers produce useful but limited data such as static and dynamic characteristics but when fused with gyroscopes could deliver relative heading/direction. Sensor fusion often equated to bulky devices, but micro-electromechanical systems (MEMS) facilitated new synchronized/unsynchronized data collection possibilities with discrete wearable technologies. This has enabled more pragmatic multi-modal sensor fusion to provide real-world and clinically relevant information to increase utility and accuracy of rehabilitation systems. For example, fusion approaches have seen acceleration signals fused with electrocardiography (ECG) signals to calculate energy expenditure [48] and electromyography (EMG) signals to monitor functional activities in stroke survivors [49]. However, studies generally rely on gait data gathered indoors within a controlled environment only.

Development of any multi-modal fusion approach needs to examine the methodology in laboratory and free-living based environments. This is important as previous research reported that gait adaptation techniques for maintaining stability are affected by walking terrain [50]. The impact of environment has been investigated in uni-modal gait studies for neurological conditions, and significant spatio-temporal differences were revealed between

indoor and outdoor/free-living environments [51, 52]. However, understanding potential reasons for poor mobility and falls is limited since additional gait characteristics (i.e., kinematic joint angles and muscle activation) were not previously included. Additionally, outdoor studies focused on activity recognition or activity level tracking rather than specific gait characteristics. For example, a study proposed an ECG, skin conductance, respiration and gait acceleration signals-based gait monitor system for habitual environments, but failed to include clinically relevant lower limb gait characteristics such as spatio-temporal, kinematic and muscle activation [53].

Therefore, the proposed novelty of this study is to investigate multi-modal gait characteristics in both clinical/lab and habitual environments by proposing a novel multi-layer fusion approach along with synchronized IMU and EMG. Although existing chosen wearable algorithms are individually validated for a single gait outcome, these algorithms have not been fused for the purposes outlined here. Multi-modal investigation of neurological gait with clinically relevant characteristics in natural habitats remains lacking, perhaps due to the shortage of developments in the field. Here, we utilise a multi-modal wearable to implement a novel fusion approach consisting of validated algorithms and synchronized sensor data for use in the lab/clinic and beyond such as outdoor level walking, incline walking, stair ascent/descent. Preferred algorithms and locations were chosen based on their performances that were investigated in the literature [11, 38, 54-56] and as part of investigative developments conducted within this study. We hypothesis that the proposed work can better inform gait assessment through adoption of a multi-layer fusion approach (wearables/sensors, algorithms and gait characteristics). Therefore, main contributions of this study are to:

i. develop a framework that fuses validated wearable-based gait algorithms for multi-modal gait assessment use in laboratory and free-living environments,
ii. examine implementation by investigating use on a cohort of healthy adults and,
iii. investigate use within a pilot study of SS to evidence clinical effectiveness for use beyond the clinic/lab, revealing impact of different terrains and activities on spatio-temporal, kinematic and muscle activation,
iv. provide insight to limitations with existing algorithms

The fusion methodology provided here will showcase how multi-modal gait assessment can be created which could enable clinicians to prepare more informed rehabilitation programs and measure their effectiveness. Section 2 summarises the experimental protocol including participant demographics, data collection protocol and performed gait tasks. Section 3 contains various algorithms adopted here and provide details about pre-processing, used signal, sensor orientation and multi-layer data fusion framework. Section 4 presents the results extracted from the framework, including indoor, outdoor level walking multi-modal gait characteristics and impacts of changing environments for both healthy population and stroke survivors. Experimental results of walking on the rocky surface, incline walking and stair ambulation are provided in supplementary materials. Section 5 present discussions about the multi-modal approach, implementation, and limitations. Finally, conclusions are given in section 6.

2. Experimental protocol

2.1. Participants

Ten healthy participants (HP's) were recruited for the main study (28.4 ± 7.0yrs, 79.2 ± 14.4kg, 176.8 ± 8.4cm, 8M:2F) and three SS (72.3 ± 3.1yrs, 78.5 ± 12.1kg, 176 ± 8.2cm, 3M, right side most affected for all) for the clinical pilot. Assessment and instrumentation were carried out by a physiotherapist and trained researchers, respectively. Ethical consent was granted by the Northumbria University Research Ethics Committee (REF: 21603). All participants gave informed written consent before participating in this study. Testing took place at the Clinical Gait Laboratory, Coach Lane Campus, Northumbria University, Newcastle upon Tyne.

2.2. Data collection and gait tasks

Each participant wore four Shimmer3 EMG wearables (24.9cm^3, 31g) with straps on the lateral side of the thighs and shanks, approximately 7-8 cm above the ankle and knee joints, respectively, (Figure 1, S). Before data collection, wearables attached to the shank and thigh level were positioned in the same vertical line while participant stood still to achieve a better knee flexion angle estimation. The wearable enables multi-modal capture of IMU and EMG data simultaneously. Signals were recorded at a sampling frequency of 512Hz, and IMU configured (16-bit resolution, ±8g, ±500°/s) prior to data collection. Skin preparation for EMG electrode attachment was performed with alcohol swabs to achieve better skin-electrode contact. Disposable surface electrodes (circular - Ag/AgCI, silver/silver chloride) were placed bilaterally (inter-electrode spacing ≈30mm) on clean skin according to SENIAM recommendations and locations: rectus femoris (**RF**), biceps femoris (**BF**), tibialis anterior (**TA**) and gastrocnemius (**GS**), with a reference electrode on the ankle and knee. In each wearable (worn on the left and right legs), channel 1 (ch1) was assigned to TA and RF muscle groups for shank and thigh

level sensors, respectively. Similarly, channel 2 (ch2) was assigned to GS and BF muscle groups for shank and thigh level sensors, respectively.

Each participant was instructed to walk over ground for 2-minutes around a 20m circuit at their preferred self-selected walking speed inside the laboratory. Subsequently, participants walked outdoors with the same wearables. Outdoor walking consisted of a pre-defined route, including ground level walking on different surfaces (e.g., asphalt, uneven rock, pavement) (Figure 1, F1-F2-F3), inclined walking (wheelchair ramp) (Figure 1, F4), ascending/descending stairs (Figure 1, F5-F6), with a physiotherapist and trained researcher (approx. 20 min). For safety, walking on an uneven rock surface and inclined walking on a wheelchair ramp were excluded for SS. Two-minute data recorded inside and outside (on asphalt and pavement) during level walking are presented here (additional walking surface data available online).

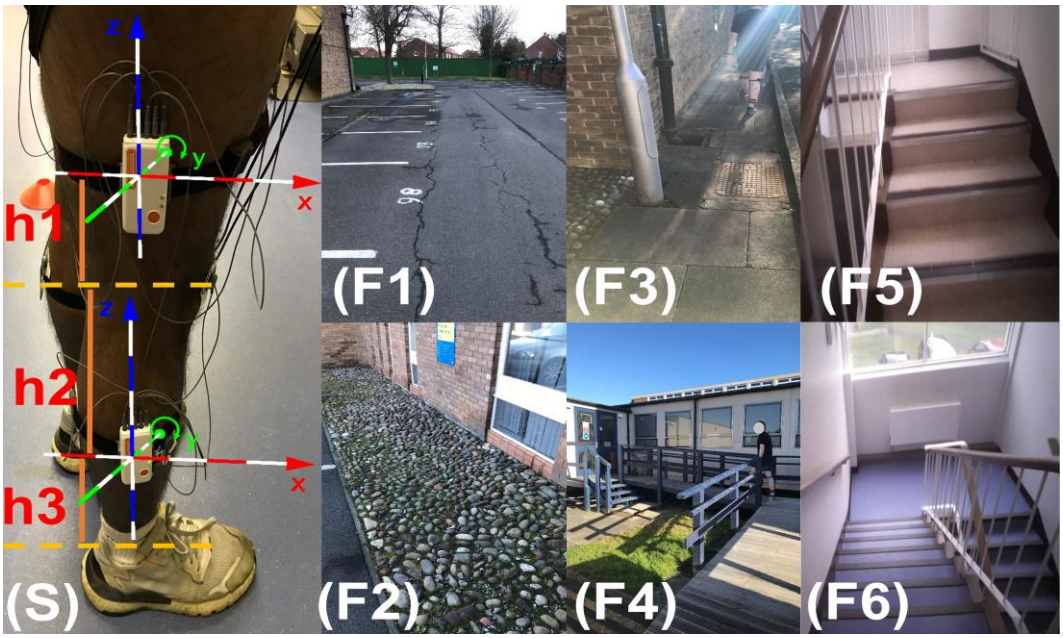

Figure 1. Sensor placement and physical tasks. (S) sensor placement illustration, (F1, F2 and F3) free living walking on asphalt, uneven rock surface and pavement, (F4, F5 and F6) free living incline walking, stair ascent and stair descent, respectively.

3. Methodology

Here we present the proposed multi-layered fusion approach by combining validated algorithms, multi-modal sensors, inertial and EMG data culminating in many gait characteristics. IMU and EMG data were transferred to a workstation (Windows 10) from the wearable via proprietary software (Consensys). Custom programs in MATLAB® (2019, Statistics and Machine Learning Toolbox, MathWorks, Inc., Natick, US) analysed raw (sample level) IMU and EMG data for spatio-temporal, kinematic and EMG analysis. Stride time was calculated as the average of left and right strides. All spatio-temporal gait characteristic results are presented similar to clinical domains of gait (pace, rhythm, variability and asymmetry) [29, 57].

Various validated algorithms (***A***) were selected to extract informative multi-model gait characteristics. Of critical importance within the suggested approach are initial contact (IC i.e., heel strike) and final contact (FC i.e., toe-off) times for right and left foot derived from the shank mounted wearables. IC and FC events help segment the gait cycle and denote specific regions of interest. Walking periods on different terrains and stair ambulation were manually segmented based on the pre-defined route and time stamps. Participants were asked to stand still for five seconds before and after each activity for more accurate manual segmentation. A general logical flow is presented in Figure 2 and broadly described as follows:

- IC and FC were extracted with two different algorithms. Ground level IC-FC times were detected with (algorithm) 1 (***A1)*** [18], whereas incline walking, stair ascent & descent IC-FC times were detected with ***A2*** [20, 21]. Only step time is calculated using the synchronised left and right shank IMU sensor timestamps. The remaining spatio-temporal parameters are calculated from the right shank sensor for the right side and the left shank sensor for the left side.
- Spatial characteristics (stride velocity and stride length) were estimated using ***A3*** [23] and IC-FC times of ***A1*** *and* ***A2***, depending on activity (e.g. level walking or incline walking)
- Knee flexion angle and muscle activation for each stride were segmented considering the type of activity.

For example, knee flexion angles during ground level and incline walking were estimated using ***A4*** [39] and ***A1***, while knee flexion angles for stair ascent & descent were estimated with ***A5*** [40] and ***A2***.

- Muscle activation (bursts) patterns were extracted using k-means approach ***A6*** [44] together with ***A1*** (for ground level walking and incline walking) and ***A2*** (for stair ascent & descent), Figure 2.

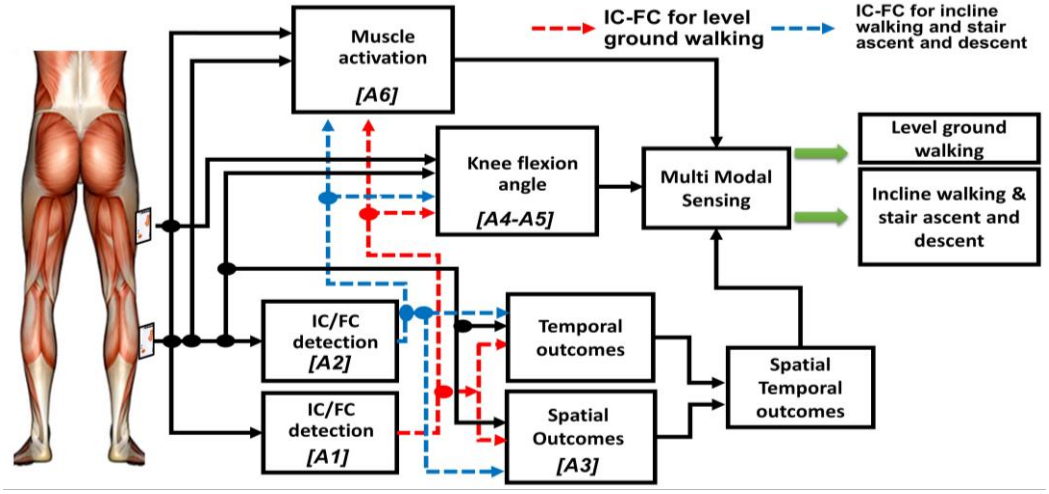

Figure 2. General flow chart (left to right) of the sensor and data fusion framework, ***A*** for algorithm used. This details the fusion approach for the right leg only, the same is repeated for the left mounted multi-modal wearables.

3.1. Data pre-processing

Appropriate filtering must be performed to ensure all sensor signals are physiological related and not corrupted by noise [58]. For example, previous studies reported that during barefoot walking, 99% of the acceleration signal is contained frequency below 16 Hz [59, 60]. Thus higher frequencies are filtered out in the majority of the gait studies[61]. Here, various pre-processing algorithms (Table 1) were applied to raw sensor data depending on the parameter to be extracted as detailed in validation studies:

- IC-FC during level walking: a multi-resolution wavelet decomposition was applied on raw angular velocity signal (perpendicular to the sagittal plane), drift and high-frequency artefacts were cancelled by obtaining an approximation, ***A1***. A digital filter (second-order Butterworth low pass filter with a cut off frequency of 35Hz) was applied to the collected angular velocity signal to smooth the signal prior to detection of IC and FC during incline walking and stair ascending & descending, ***A2***.
- Spatial parameters: Accelerometer and gyroscope signals were filtered (first-order Butterworth low pass filter with a cut off frequency of 5Hz) to cancel high frequency components before the estimation of step velocity from shank mounted sensor. Additionally, the angular velocity signal was filtered (first-order Butterworth low pass filter with a cut off frequency of 0.001Hz) to reduce integration drift, ***A3***.
- Knee joint flexion: A third-order Savitzky–Golay filter was applied to smooth the accelerometers and gyroscopes signals before the extraction of knee joint angles, ***A4***. Both physical sensors' signals attached to shanks and thighs were filtered (fourth-order Butterworth low pass filter with a cut off frequency of 4 Hz) prior to the estimation of sensor orientation, consequently calculation of the joint angle in **A5**.
- EMG: A zero-lag fourth-order bandpass Butterworth filter with cut-off frequencies of 20Hz and 250Hz was applied to EMG data, followed by rectification, and a second zero-lag fourth-order Butterworth low-pass filtering at 6Hz, **A6**.

Table 1: Data pre-processing

Input:	
$Sacc_{x,y,z}(i)$; $Sgyro_{x,y,z}(i)$;	*// upload Shank (S) and thigh (T) sensors, accelerometer (acc) and gyroscope(gyro) signals*
$Tacc_{x,y,z}(i)$; $Tgyro_{x,y,z}(i)$;	*// upload EMG channels ($EMG_{ch1, ch2}$) of upper(thigh) and lower (shank) leg sensors*
$S,T_{EMG\text{-}ch1, ch2}$;	
Fs=512;	*// sampling frequency (Fs)*
Filtering:	
$Sgyro_y$=*wavedec*($Sgyro_y$) & *appcoef;*	*// wavelet decomposition and approximation (coif5)-**A1***
$Sgyro_y$=*lpf* ($Sgyro_y$);	*// low pass filtering (lpf)-**A2***
$Sacc_{x,z}$,$Sgyro_y$= *lpf,hpf* ($Sacc_{x,z}$,$Sgyro_y$);	*// low pass filtering (lpf)- high pass filtering (hpf)- **A3***
$S,Tacc_{x,z}$,$S,Tgyro_y$= *sgf* ($S,Tacc_{x,z}$,$S,Tgyro_y$);	*// Savitzky–Golay filtering (sgf)-**A4***
$S,Tgyro_y$=*lpf* ($S,Tgyro_y$);	*// low pass filtering (lpf)-**A5***
$S,T\text{-}EMG_{ch1, ch2}$=*bpf,lpf*($S,T\text{-}EMG_{ch1,ch2}$);	*// band pass filtering (bpf)-**A6***

3.2. Multi-modal wearable and data fusion methodology

Here, validated algorithms are fused i.e., implemented in a co-dependent arrangement to inform the identification and segmentation of the gait cycle during 2-minute indoor and outdoor walking. The fusion approach also utilises inertial data from different sensor locations (shank and thigh) to quantify kinematic data. Lastly, a range of inertial and EMG gait derived gait characteristics are presented in two different cohorts.

3.2.1. A1: IC and FC events during level walking

A previously validated algorithm was used to identify IC-FC times using shank mounted sagittal plane IMU angular velocity [18]. In brief, wavelet decomposition (5^{th} order coiflet, ten scales) was used to split the signal into low (approximation) and high frequency (details) components. Subsequently, drift and high-frequency movement artefacts were removed with an initial approximation. Then, two new approximations were obtained to enhance the detection of IC-FC events, respectively. For each approximation, the time corresponding to the global maximum (t_{ms} = time of mid-swing) of the signals were detected. Finally, IC-FC events (negative peaks) were searched (local minima) in predetermined intervals [IC (t_{ms}+0.25s, t_{ms}+2s), FC (t_{ms}-2s, t_{ms}-0.05s)].

A1: IC-FC detection and temporal gait characteristic estimation during level walking	
Input:	
$Sgyro_{y\text{-}r,l}(i)$;	*// upload right and left shank angular velocities*
Fs=512;	*// sampling frequency (Fs)*
Procedure:	
1. *$a_{2,3}$=get two new approx.*	
2. ***for*** *i=1: N*	*// (1: N=sample number at the end of walking period), mid-swing (ms)*
3. *$msIC_{r,l}$=find global max points (a_2);*	*// reference points for detecting ICs*
4. *$msFC_{r,l}$=find global max points (a_3);*	*// reference points for detecting FCs*
5. ***end for***	
6. ***for*** *i=1: numel(a2)*	
7. *ICs-$_{r,l}$=find local minima [msIC+0.25s, msIC+2s]*	*// saving initial contact times*
8. ***end for***	
9. ***for*** *i=1: numel(a3)*	*// saving final contact times*
10. *FCs-$_{r,l}$ =find local minima [msFC-2s, msFC-0.05s]*	
11. ***end for***	*// temporal parameter estimations*
12. ***for*** *i=1: numel(ICs+1)*	
13. *stance(i)-$_{r,l}$=FCs(i+1)-ICs(i);*	
14. *swing(i)-$_{r,l}$=ICs(i+1)-FCs(i+1);*	
15. *stride(i)-$_{r,l}$=ICs(i+1)-ICs(i);*	
16. *rstep(i)= rIC(i)-lIC(i)*	*// right/left step time are estimated using timestamp information of right/left IC-FC times*
17. *lstep(i)= lIC(i+1)-rIC(i)*	
18. ***end for***	
19. *StepTimeVar=sqrt((var(rstep)+ var(lstep))/2);*	
20. *StepTimeAsym = abs(mean(lstep)–mean(rstep));*	*// variance calculation*
Output: *rIC, rFC, lIC, lFC;*	*// asymmetry calculation*
stance times-$_{r,l}$;swing times-$_{r,l}$;stride times-$_{r,l}$;step times-$_{r,l}$;	

3.2.2. A2: IC and FC events during inclined walking and stair ascent or descent

Formento *et al*. validated an algorithm for IC-FC detection during inclined walking [20] and stair ascent or descent [21]. Similar to ***A1***, IC-FC events were estimated based on the detection of two negative peaks considering the swing period as a reference point in the shank angular velocity signal. In the ***A1***, IC-FC events were searched in predetermined intervals, whereas, in ***A2***, these events were detected based on a set of predetermined rules. Briefly, the algorithm begins with searching the swing phase of a gait cycle. When the gyroscope signal exceeds a predetermined threshold for at least 40 milliseconds, the algorithm considers the swing phase is detected. Then, the first negative minimum after swing phase is defined as IC. Around the time of IC, the gyroscope signal may present further negative peaks related to events during the loading response. In order to avoid false FC detection during that time, a "waiting time" was set during which there was no search for FC events. The waiting time was set to be 50% of the duration of the positive wave for the first step analysed and 50% of the last stance phase for the remaining steps. Once waiting time is over, FC is defined as the sample that represents a minimum negative peak in a window of 200ms, that is preceded by a decreasing (more negative angular velocity) trend in the signal and followed by an increasing (more positive voltage) trend.

A2: IC-FC detection and temporal gait characteristic estimation during incline walking and stair ascent or descent	
Input:	
$Sgyro_{y\text{-}r,l}(i)$;	*// upload right and left shank angular velocities*
Fs=512;	*// sampling frequency (Fs)*
Procedure:	
1. ***for*** *i=1: N*	
2. *ms=find global max points ($Sgyro_{y\text{-}r,l}$);*	*// (1: N= sample number at the end of walking period), mid-swing (ms)*
3. ***end for***	*// reference points for detecting ICs and FCs*

4.	***for*** *i=1: numel(ms)*	
5.	*ICs $_{r,l}$ =find local minima after [ms]*	
6.	*set waiting time*	*// saving initial contact times*
7.	*FCs $_{r,l}$ = find following local minima after waiting time*	
8.	***end for***	*// saving final contact times*
9.	***for*** *i=1: numel(ICs+1)*	
10.	*stance(i) $_{r,l}$ =FCs(i+1)-ICs(i);*	*// temporal parameter estimations*
11.	*swing(i) $_{r,l}$ =ICs(i+1)-FCs(i+1);*	
12.	*stride(i)-$_{r,l}$=ICs(i+1)-ICs(i);*	
13.	*rstep(i)= rIC(i)-lIC(i)*	*// right/left step time are estimated using timestamp information of right/left IC-FC times*
14.	*lstep(i)= lIC(i+1)-rIC(i)*	
15.	***end for***	
Output: *rIC, rFC, lIC, lFC;*		
stance times-$_{r,l}$;swing times-$_{r,l}$;stride times-$_{r,l}$;step times-$_{r,l}$;		

3.3. A3: Spatial parameter extraction during ground level walking

A validated algorithm (***A3***) [23] was used to estimate spatial parameters (stride velocity) from shank mounted IMU. The algorithm is an improved and simplified version of [22], where both horizontal and vertical accelerations were considered. As only horizontal velocity and displacement are needed, acceleration and angular velocities in the sagittal plane (the plane of progression) were considered, vertical components were excluded.

First, gait cycles were segmented from mid-stance to mid-stance (unlike ***A1*** and ***A2***) based on the assumption that the velocity of the shank is zero in the moment of mid-stance, the moment when the shank is parallel to the direction of gravity. Then, the angular velocity signal was integrated to calculate Θ for each gait cycle, Eq. 1. Afterwards, horizontal acceleration components of the sensor's coordinate system were calculated for the global coordinate system using calculated Θ (Eq.2). Finally, horizontal velocity was computed with the integration of horizontal acceleration and corrected with the horizontal velocity component Eq. 3. Horizontal correction velocity ($V_{hor\text{-}correction}$) component was calculated considering the initial horizontal speed at the start of the stride and the distance (Figure 1, *h3*) between the ankle joint and shank wearables. Finally, the stride length is calculated by multiplication of corrected horizontal stride velocity and stride time (estimated temporal parameter) for each gait cycle, Eq. 4. Results of the developed algorithm suggest that the distance between the shank mounted wearable and the ankle (*h3*) has a negligible impact (± 2cm) on the accuracy of the measure [23]. Study findings also reported that the effects of numerical drifts are insignificant as integrations are performed for a short period of time - only gait cycle (max 1.4s).

$$\theta(t) = \int_0^{t_{end}} \omega_s(t)dt \tag{1}$$

$$a_{hor}(t) = \cos\theta(t)ax(t) - \sin\theta(t)az(t) \tag{2}$$

$$v_{hor}(t) = \int_0^{t_{end}} a_{hor}(t)dt + v_{hor-correction} \tag{3}$$

$$Stride\_length = v_{hor}\ x\ stride\_time \tag{4}$$

where, θ and ω_s are orientation angle and shank angular velocity, respectively. The a_{hor}, v_{hor} and t are horizontal acceleration, velocity, and the duration represents stance to stance period, respectively.

A3: Stride length and velocity estimation		
Input:		
Sacc$_{x,\ z\text{-}r,l}$(i); Sgyro$_{y\text{-}r,l}$(i);		*// upload right and left shank accelerations and angular velocities*
Fs=512;		*// sampling frequency (Fs)*
Procedure:		
1.	***for*** *i=1: numel(rIC-lIC)*	
2.	*find mid-stance= max (Sgyro$_{y\text{-}r,l}$ (ICs $_{r,l}$(i): FCs $_{r,l}$(i+1)))*	*// segmenting relevant signals from mid stance to mid stance for a stride using timestamp information of ICs and FCs*
3.	*segmented_ Sacc$_{x,\ z\text{-}r,l}$ (i)= Sacc$_{x,z\text{-}r,l}$ (mid-stance(i): mid-stance (i+1));*	
4.	*segmened_ Sgyro$_{y\text{-}r,l}$ (i)= Sgyro$_{y\text{-}r,l}$ (mid-stance(i): mid-stance (i+1));*	
5.	***end for***	
6.	*segmened_ Sgyro$_{y\text{-}r,l}$ =deg2rad(segmened_ Sgyro$_{y\text{-}r,l}$)*	*// convert angle from degrees to radians*
7.	*theta (i)= integration of segmented_Sgyro $_{y\text{-}r,l}$ (i);*	*// calculation of the orientation of the sensor across a stride*
8.	*costheta=cos(theta); sintheta=sin(theta);*	
9.	***for*** *i=1: numel(theta)*	
10.	*ahor$_{r,l}$ (i)= costheta(i)* Sacc$_x$(i)- sintheta(i)* Sacc$_z$(i);*	*// estimation of horizontal acceleration in world coordinate system*
11.	***end for***	
12.	*vhor $_{r,l}$= integration of ahor$_{r,l}$ +vhor$_{correction}$*	*//calculation of the velocity and displacement across a stride*

13. *Stride_length=mean(vhor)*stride_time*
14. ***Output:*** *vhor$_{r,l}$; Stride_length $_{r,l}$;*

3.4. Kinematic angles

3.4.1. A4: Knee angle estimation during level walking

Kinematic joint angles are typically calculated from the orientations of IMU wearables that are estimated either using gravitational acceleration or integrated angular velocity [40]. In the latter, error (drift) may occur due to integration. One method to avoid integration drift is to use neural networks, which require training from sufficient data involving a large number of participants [62]. Kalman filtering is another approach, but three dimensional orientation errors reported [63]. However, in the former approach, it is possible to estimate the orientation of sensors by the gravitational acceleration in static states, but in dynamic states like gait, translational acceleration will be included.

Takeda *et al*. [39] developed an algorithm (a simplified version of [41]) considering measurements at the centre of a proposed link model. The developed algorithm estimates knee flexion angles for a dynamic state (level walking) after elimination of translational acceleration. Here, [39] was replicated to estimate knee flexion angles. First, each stride was segmented from continuous walking using IC-FC estimations (***A1)***. Then, segmented acceleration and angular velocity signals from each left and right thigh and shank were used to estimate knee flexion. For the purposes of this study, angular velocity and the sensor distance from knee was used to calculate the translational acceleration during gait, Eq5. The estimated translational acceleration was then subtracted from the measured acceleration data to obtain the gravitational acceleration. The gravitational acceleration provided the orientation angle of the segments and, consequently, the three-dimensional posture of lower limb segments, Eq. 6. Once the orientation of each segment was calculated, knee flexion was estimated by the difference between the angle of inclination of shank and thigh, Eq. 7.

$$\ddot{r}_{KS} = \dot{\omega}_S \times r_{KS} + \omega_S \times (\omega_S \times r_{KS}) \,,\ \ddot{r}_{KT} = \dot{\omega}_T \times r_{KT} + \omega_T \times (\omega_T \times r_{KT}) \quad (5)$$

where $\ddot{r}_{KS}$ and $\ddot{r}_{KT}$ are calculated translational accelerations for shank and thigh sensors, respectively. ω_S and ω_T are angular velocity signals of shank and thigh sensors, r_{KS} and r_{KT} are the distance of the attached sensors from knee (Figure 1, h1-h2).

$$\theta_1 = \arctan(|O_T - \ddot{r}_{KT}|_x / |O_T - \ddot{r}_{KT}|_z) \quad \theta_2 = \arctan(|O_S - \ddot{r}_{KS}|_x / |O_S - \ddot{r}_{KS}|_z) \quad (6)$$

$$\theta_{Flexion} = \theta_2 - \theta_1 \quad (7)$$

where O_S and O_T are raw acceleration outputs of sensors.

A4: Knee joint flexion-extension angle estimation

Input:
Sacc$_{x,\ z\text{-}r,l}$(i); Sgyro$_{y\text{-}r,l}$(i); Tgyro$_{y\text{-}r,l}$(i); Tacc$_{x,\ z\text{-}r,l}$(i); — *// upload right and left shank accelerations and angular velocities*
Fs=512; — *// sampling frequency (Fs)*
Procedure:
1. ***for*** *i=1: numel(rIC-lIC)*
2. *segmented_ Sacc$_{x,\ z\text{-}r,l}$(i)= Sacc$_{x,\ z\text{-}r,l}$(ICs $_{r,l}$(i): ICs $_{r,l}$(i+1));*
3. *segmened_ Sgyro$_{y\text{-}r,l}$(i)= Sgyro$_{y\text{-}r,l}$(ICs $_{r,l}$(i): ICs $_{r,l}$(i+1));*
4. *segmented_ Tacc$_{x,\ z\text{-}r,l}$(i)= Tacc$_{x,\ z\text{-}r,l}$(ICs $_{r,l}$(i): ICs $_{r,l}$(i+1));*
5. *segmened_ Tgyro$_{y\text{-}r,l}$(i)= Tgyro$_{y\text{-}r,l}$(ICs $_{r,l}$(i): ICs $_{r,l}$(i+1));*
// segmenting relevant signals for a stride using timestamp information of right and left ICs and FCs
6. ***end for***
7. *segmened_ S,Tgyro$_{y\text{-}r,l}$ =deg2rad(segmened_ S,Tgyro$_{y\text{-}r,l}$)* — *// convert angle from degrees to radians*
8. $\ddot{r}_{KS}$ *(i)= diff (segmened_ Sgyro$_{y\text{-}r,l}$).r_{KS} + segmened_ Sgyro$_{y\text{-}r,l}$. (segmened_ Sgyro$_{y\text{-}r,l}$. r_{KS});* — *// calculation of translational accelerations*
9. $\ddot{r}_{KT}$ *(i)= diff (segmened_ Tgyro$_{y\text{-}r,l}$).r_{TS} + segmened_ Tgyro$_{y\text{-}r,l}$. (segmened_ Tgyro$_{y\text{-}r,l}$. r_{KT});*
10. *theta$_1$= atan((abs(Tacc$_{-r,l}$ -* $\ddot{r}_{KT}$ *))$_x$ / (abs(Tacc$_{-r,l}$ -* $\ddot{r}_{KT}$ *))$_z$);* — *// estimation of orientation angle of shank and thigh sensors*
11. *theta$_2$= atan((abs(Sacc$_{-r,l}$ -* $\ddot{r}_{KS}$ *))$_x$ / (abs(Sacc$_{-r,l}$ -* $\ddot{r}_{KS}$ *))$_z$);*
12. *theta$_{F\text{-}E}$=theta$_2$-theta$_1$* — *// calculation flexion extension angle*
13. *theta$_{F\text{-}E}$ = rad2deg(theta$_{F\text{-}E}$)* — *// convert angle from radians to degree*
Output: *theta$_{F\text{-}E}$*

3.4.2. A5: Knee angle estimation during inclined walking, stair ascent and descent

Nestares and Callupe developed an algorithm based on orientations of shank and thigh level sensors to evaluate

knee joint angle during level walking and stair ascent on HP and SS [42]. The study reported that shank and thigh level sensors' orientation could compute knee flexion angles with high accuracy during level walking and stair ambulation. The developed algorithm used a complementary filter to estimate sensor orientations. However, it was reported that the fusion coefficient of a complementary filter is too sensitive to be pragmatically used and thus requires additional operations [64]. An alternative and more practical way of estimating sensor orientation is integrating angular velocity as suggested by Tong *et al.* [40] (during level walking).

Here, a novel application of both algorithms was utilised for the purpose of this study to achieve a practical knee flexion angle estimation algorithm during incline walking and stair ambulation. First, each stride was segmented from continuous walking using ICs and FCs (***A2)***. Then shank and thigh sensor angular velocities were integrated to estimate sensor orientation (inclination) across a stride, Eq. 8. Finally, the knee angle was calculated by subtracting the inclination (orientation angle) of the thigh from the inclination of the shank, Eq. 9 (similar to ***A4*** Eq.7).

$$\theta(t)_S = \int_0^{t_{end}} \omega_S(t)dt\,,\ \theta(t)_T = \int_0^{t_{end}} \omega_T(t)dt \tag{8}$$

$$\theta_{F-E} = \theta_S - \theta_T \tag{9}$$

where ω_S , ω_T and t are angular velocities measured from shank and thigh sensors and gait cycle period (stride time), respectively.

A5: Knee joint flexion-extension angle estimation	
Input:	
Sgyro$_{y\text{-}r,l}$(i); Tgyro$_{y\text{-}r,l}$(i);	*// upload right and left shank angular velocities*
Fs=512;	*// sampling frequency (Fs)*
Procedure:	
1. ***for*** *i=1: numel(rIC-lIC)*	
2. *segmened_ Sgyro$_{y\text{-}r,l}$(i)= Sgyro$_{y\text{-}r,l}$(ICs$_{r,l}$(i): ICs$_{r,l}$(i+1));*	*// segmenting relevant signals for a stride using timestamp information of ICs and FCs*
3. *segmened_ Tgyro$_{y\text{-}r,l}$(i)= Tgyro$_{y\text{-}r,l}$(ICs$_{r,l}$(i): ICs$_{r,l}$(i+1));*	
4. ***end for***	
5. *segmened_ S,Tgyro$_{y\text{-}r,l}$ =deg2rad(segmened_ S,Tgyro$_{y\text{-}r,l}$)*	*// convert angle from degrees to radians*
6. *theta$_1$ (i)= integration of segmented_Tgyro $_{y\text{-}r,l}$ (i);*	*// estimation of orientation angle of shank and thigh sensors*
7. *theta$_2$ (i)= integration of segmented_Sgyro $_{y\text{-}r,l}$ (i);*	
8. *theta $_{F\text{-}E}$=theta$_2$-theta$_1$*	*// calculation flexion extension angle*
9. *theta $_{F\text{-}E}$ = rad2deg(theta$_{F\text{-}E}$)*	*// convert angle from radians to degree*
Output: *theta$_{F\text{-}E}$*	

3.5. A6: EMG muscle activity (burst) detection

Detection of muscle activity/inactivity and overall level of activity in a muscle at any time is relatively identifiable from the linear envelope of raw EMG signals. There are various methods to extract the linear envelope of EMG signal such as root mean square (RMS), mean of moving window, and use of a set of filters along with rectification [65, 66]. Once the linear envelope is extracted, muscle activity/inactivity can be detected via a predetermined threshold, manual observation, or clustering algorithms[67]. The latter finds resemblances between data points and groups these according to their similarities.

Here, the filters described in Section 3.1 (***A6***) and full-wave rectification were used to extract the linear envelope of the EMG signal, while k-means clustering was used to search muscle bursts (activity). The rationale for k-means is that it does not require a priori setting of thresholds for each individual and has shown the ability to differentiate burst, even when bursts are short or have spike-like characters [68]. Similar to [44], each data point in the EMG linear envelopes are clustered into subsets of data using k-means. Then, EMG signals are dichotomised into periods of activity and inactivity according to the amplitude of each data point. Here, the numbers of centroids (clusters), which influence sensitivity, were set to five after visual inspection for all EMG signals analysed. Muscle inactivity is identified for the lowest two clusters, whereas the remaining three clusters are accepted as muscle activity. All EMG values for each participant underwent time normalisation within the gait cycle and amplitude normalisation to the highest EMG value in the gait cycles.

A6 Muscle burst detection via k-means clustering	
Input:	*//upload EMG channels (EMG$_{ch1,\ ch2}$) of upper(thigh) and lower leg (shank) sensors*
S,T-$_{EMG\text{-}ch1,\ ch2}$;	
Fs=512;	*// sampling frequency (Fs)*
Procedure:	
1. ***for*** *i=1: numel(rIC-lIC)*	*// segmenting relevant signals for a stride using timestamp information of ICs and FCs*
2. *segmened_ S$_{EMG\text{-}ch1,\ ch2\text{-}r,l}$(i)= S$_{EMG\text{-}ch1,\ ch2\text{-}r,l}$(ICs$_{r,l}$(i): ICs$_{r,l}$(i+1));*	
3. *segmened_ T$_{EMG\text{-}ch1,\ ch2\text{-}r,l}$(i)= T$_{EMG\text{-}ch1,\ ch2}$;-$_{r,l}$(ICs$_{r,l}$(i): ICs$_{r,l}$(i+1));*	
4. ***end for***	

5.	*[idx_segmened_$S_{EMG\text{-}ch1,ch2\text{-}r,l}$,mean_val]*	*// k-means clustering (# of cluster is five)*
6.	*=kmeans (segmened_S,$T_{EMG\text{-}ch1,\ ch2\text{-}r,l}$,5);*	*// sort calculated mean value (descend)*
7.	*mean_val= sort(mean_val,'descend');*	
8.	***for** i=1: numel (segmened_ S,$T_{EMG\text{-}ch1,\ ch2\text{-}r,l}$)*	*// find muscle activation if EMG envelope value is greater than lowest two mean values*
9.	***if** segmened_S,$T_{EMG\text{-}ch1,\ ch2\text{-}r,l}$ (i)<mean_val1(4)*	
10.	*kmeans_S,$T_{EMG\text{-}ch1,\ ch2\text{-}r,l}$ (i)=muscle_off;*	
11.	***else***	
12.	*kmeans_S,$T_{EMG\text{-}ch1,\ ch2\text{-}r,l}$ (i)=muscle_on;*	
13.	***end if***	
14.	***end for***	
Output:	*kmeans_S,$T_{EMG\text{-}ch1,\ ch2\text{-}r,l}$*	

4. Results

This novel fusion approach quantifies and contrasts temporal, spatial, knee joint kinematics, and muscle activation characteristics in (i) HP's during 2min walks in a lab (indoor) vs 2min outdoor walking on level ground, and (ii) in a pilot study of SS walking for 2mins, indoor vs outdoor. Here, results are deemed suitable for exploratory investigation as they are derived from well validated algorithms for use on level ground terrain. Similar modes of investigation have been conducted previously, examining uni-modal, spatio-temporal gait between clinic/lab and habitual environments [52].

Outputs of the fusion approach can be classified as; spatio-temporal, knee joint flexion and muscle activation patterns. Muscle bursts timing and durations are presented throughout the gait cycles. Multi-model gait characteristics of the left side for one HP participant (#9) during outdoor level walking were not extracted due to wearable malfunction; therefore, only mean values for the right side were calculated. IC-FC events were not detected for the paretic side of one SS participant (#3) as algorithms (***A1-A2***) failed to detect peaks due to poor gait (section 5.3); therefore, only mean values for the non-paretic side were calculated.

4.1 Healthy participants

4.1.1 Two-minute walks: Spatio-temporal, kinematics and EMG

There were differences in gait domains for spatio-temporal characteristics between indoor and outdoor walks, Table 2. Generally, participants walked with greater *pace* and *variability* but with decreased *rhythm* in outdoor compared to indoor level walking (stride length variability characteristic did not experience any changes between outdoor level walking and indoor). Among *asymmetry* characteristics, only stride length asymmetry found higher during indoor level walking compared to outdoor. There were slightly increased mean knee flexion angles (~1°) and decreased variance and asymmetry in outdoor level walking compared to indoor, Table 2. Although there are large inter-individual differences among participants, common muscle burst timing and durations patterns can be extracted via EMG signals [44], where common muscle activity patterns were observed within a gait cycle, Figure 3. Regardless of indoor/outdoor, the prevalence of TA muscle activation had similar patterns with RF and BF, all active around the start and end of a gait cycle during level walking. TA was also found active at stance to swing transition period (around FC) and throughout the swing phase in some participants. BF muscle activation was observed at the end of a gait cycle around the time of the next IC. GS prevalence was observed mostly during the later stance phase before the FC moments for push-off of the foot. (Individual data available via online supplementary material- Table S2-S3-S5).

Table 2: Multi-modal gait characteristics of healthy participants during 2-minute walks

		Indoor		***Outdoor***	
	# Mean of strides	*99.6*		*108.1*	
		Mean	*± SD*	*Mean*	*± SD*
SPATIO-TEMPORAL	**PACE**				
	Mean Stride V. (m/s)	1.174	0.127	**1.319**	0.101
	Mean Stride L. (m)	1.332	0.147	**1.415**	0.142
	RHYTHM				
	Mean Stride Time (s)	**1.136**	0.082	1.074	0.060
	Mean Step Time (s)	**0.566**	0.037	0.534	0.032
	Mean Stance Time (s)	**0.647**	0.057	0.597	0.038
	Mean Swing Time (s)	**0.489**	0.039	0.476	0.034
	VARIABILITY				
	Stride V. Var (m/s)	0.105	0.024	**0.125**	0.023
	Stride L Var (m)	**0.130**	0.041	0.129	0.029
	Step Time Var (s)	0.034	0.020	**0.039**	0.013
	Stance Time Var (s)	0.014	0.010	**0.050**	0.012
	Swing Time Var (s)	0.018	0.011	**0.043**	0.004
	ASYMMETRY				
	Stride L. Asy (m)	0.086	0.062	**0.104**	0.068

	Step Time Asy (s)	**0.033**	0.006	0.025	0.022
	Stance Time Asy (s)	**0.041**	0.010	0.012	0.008
	Swing Time Asy (s)	**0.044**	0.007	0.011	0.007
	Mean K.F.E angle	62.621°	4.229°	**63.580**°	5.220°
KNEE JOINT KINEMATICS	Variability	**5.1875**°	1.217°	4.490°	1.239°
	Asymmetry	**1.8117**°	1.040°	1.593°	1.069°

Stride V = stride velocity, Stride L = stride length. Var = variability, Asy = asymmetry
(K.F.E) knee flexion
Bold indicate greater mean values comparing indoor to outdoor.

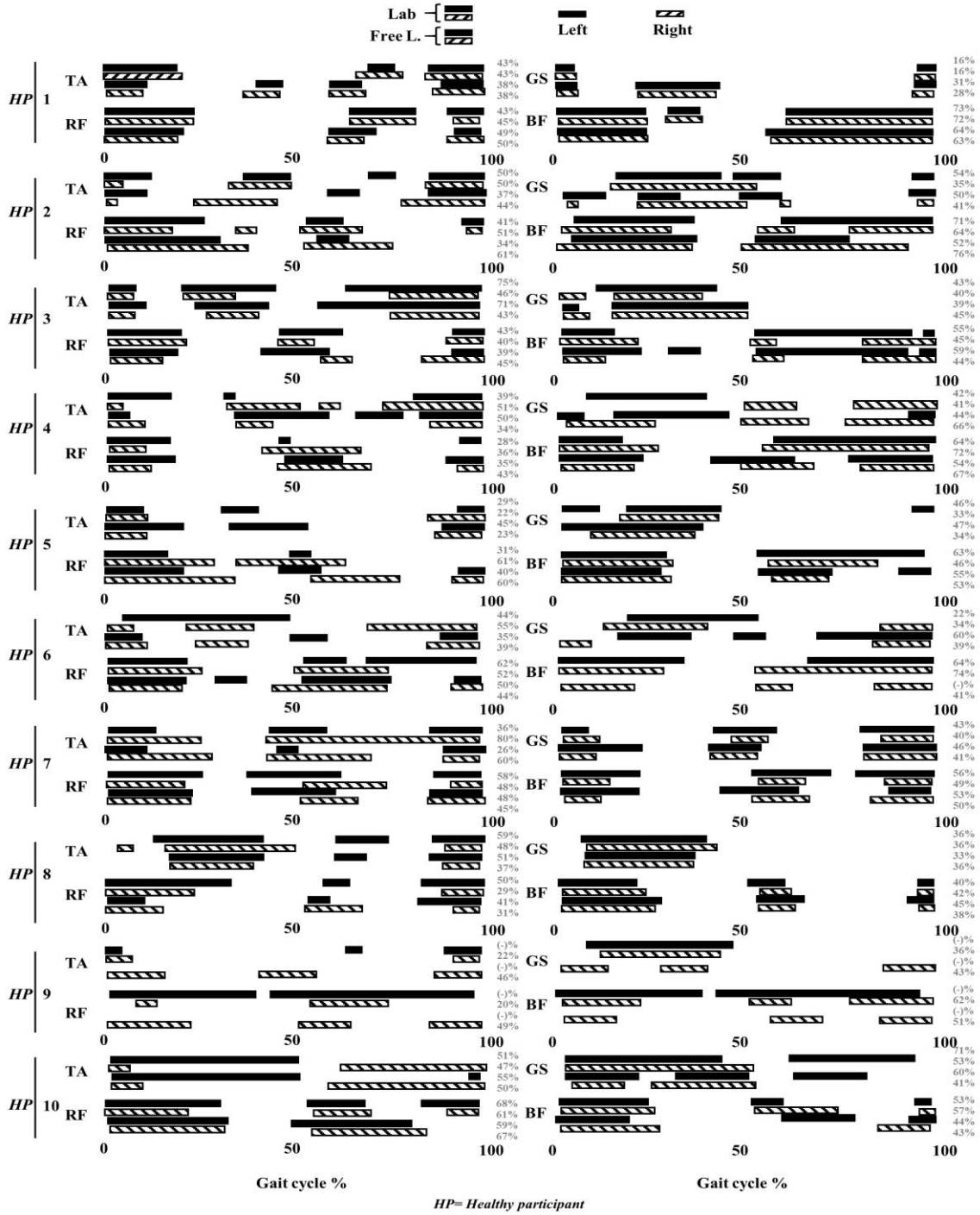

Figure 3. Muscle activity pattern healthy participants for indoor/outdoor ground level walking

4.2 Pilot study: Multi-modal gait analysis in stroke survivors

The process of extracting multi-modal gait during level walking is generally illustrated in Figure 4, highlighted here for those with stroke gait. The proposed sensor and data fusion tool provides multi-model gait characteristics during indoor and outdoor activities, but IC-FC times must be detectable initially.

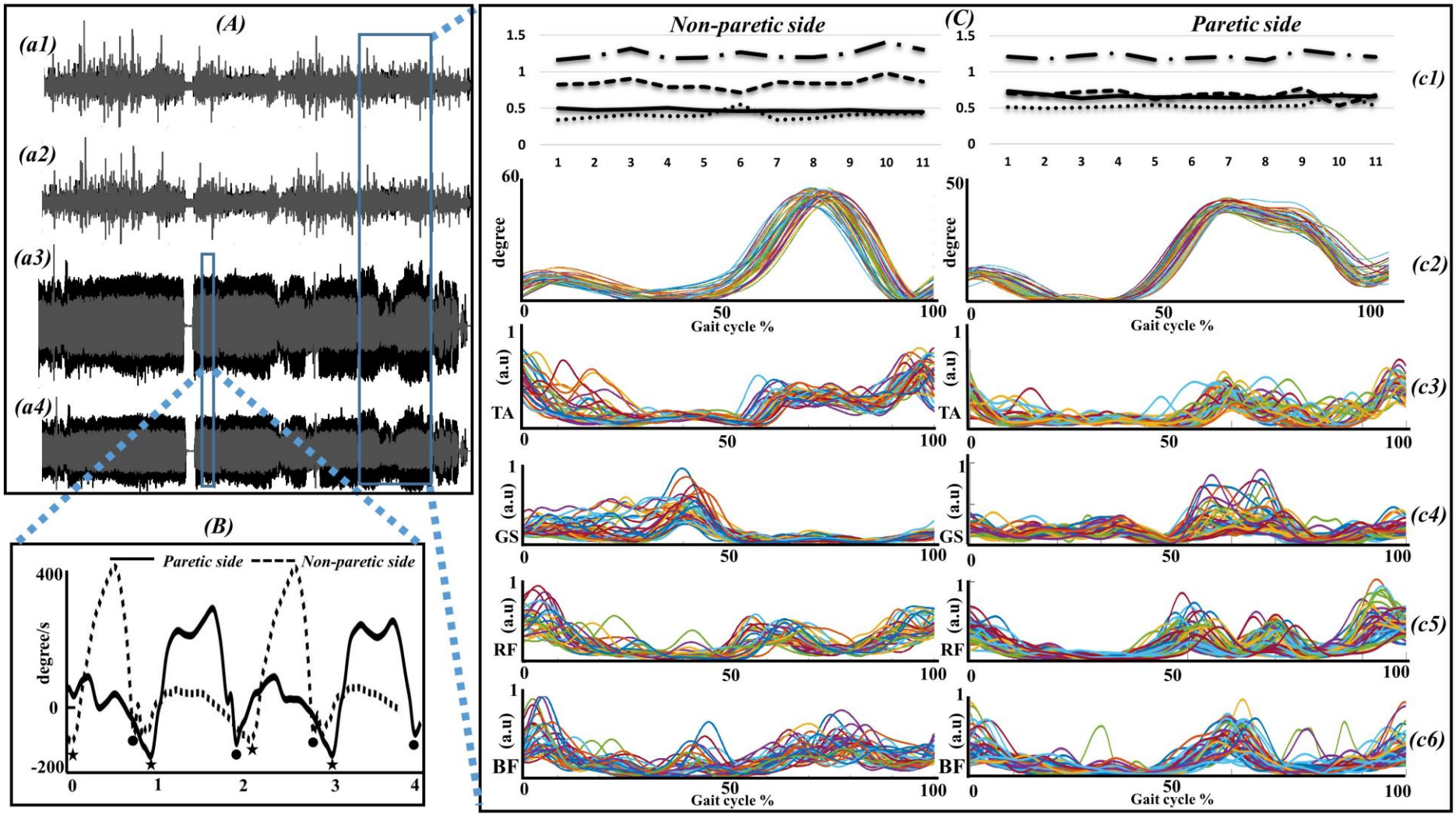

Figure 4. Level walking extracted parameters from the proposed tool. (A) Raw wearable IMU data for EMG (a1-a2) and angular velocity (a3-a4) – black represents shank mounted sensors – grey represents thigh mounted sensors, (B) Shank angular velocity of paretic and non-paretic sides: initial (dots) and final (stars) contact moments, (C) outcome of sensor fusion work for non-paretic and paretic sides: (c1) temporal characteristics where long dot dush, square dot, solid line and round dot represents (top-to-bottom) stride, stance, step and swing times respectively: (c2) estimated kinematic knee angles: (c3-c4-c5-c6) EMG activity for TA, GS, RF, and BF, respectively. a.u, Arbitrary unit-peak normalised EMG.

4.2.1 Two-minute walks: Spatio-temporal, kinematics, and EMG

Although SS presented similar shank angular velocity patterns with disturbances (e.g., oscillations) between paretic and non-paretic sides during ground-level walking, extracted indoor and outdoor temporal and spatial characteristics varied, Table 3. (Individual data available via online supplementary material- Table S4-S6-S7).
SS walked with increased *pace* and decreased *rhythm* during outdoor level walking compared to indoor. Swing time asymmetry is the only *asymmetry* characteristic that was found to be higher during indoor compared to outdoor. Among *variability*, there was no difference for stride velocity, but stance time was lower during indoor level walking compared to outdoor. (Individual and left/right data available via online supplementary material).

Noticeable differences were observed for mean, variance and asymmetry of knee joining angles. Increased mean knee flexion angles (~4°) and decreased variability and asymmetry were found during outdoor walking, compared to indoor, Table 3. Muscle activity (bursts) during indoor and outdoor walking presented in Figure 5. TA, RF and BF muscle burst were detected around the starting and ending moments of gait cycles (around IC moments). GS muscle bursts most frequently observed in the stance phase in most SS.

Table 3: Multi-modal gait characteristics of stroke survivors during 2-minute walks

		Indoor		***Outdoor***	
	# Mean of strides	*93.6*		*109.33*	
		Mean	*±SD*	*Mean*	*±SD*
SPATIO-TEMPORAL	**PACE**				
	Mean Stride V. (m/s)	1.021	0.049	**1.067**	0.119
	Mean Stride L. (m)	1.303	0.134	**1.384**	0.338
	RHYTHM				
	Mean Stride Time (s)	**1.254**	0.077	1.235	0.130
	Mean Step Time (s)	**0.614**	0.041	0.535	0.011
	Mean Stance Time (s)	**0.770**	0.085	0.748	0.142
	Mean Swing Time (s)	**0.483**	0.045	0.452	0.016
	VARIABILITY				
	Stride V. Var (m/s)	**0.189**	0.013	0.182	0.033
	Stride L Var (m)	**0.275**	0.046	0.224	0.052
	Step Time Var (s)	**0.100**	0.096	0.033	0.006
	Stance Time Var (s)	0.070	0.058	**0.074**	0.002
	Swing Time Var (s)	**0.071**	0.052	0.037	0.002
	ASYMMETRY				
	Stride L. Asy (m)	0.197	0.179	**0.290**	0.182
	Step Time Asy (s)	0.060	0.003	**0.102**	0.061
	Stance Time Asy (s)	0.063	0.001	**0.088**	0.046
	Swing Time Asy (s)	0.062	0.001	**0.067**	0.036
KNEE JOINT KINEMATICS	Mean K.F.E angle	48.120°	1.196°	**52.096°**	1.014°
	Variability	**6.064°**	0.188°	5.297°	0.660°
	Asymmetry	**22.251°**	4.506°	19.920°	6.821°

Stride V = stride velocity, Stride L = stride length. Var = variability, Asy = asymmetry
(K.F.E) knee flexion
Bold indicate greater mean values comparing indoor to outdoor

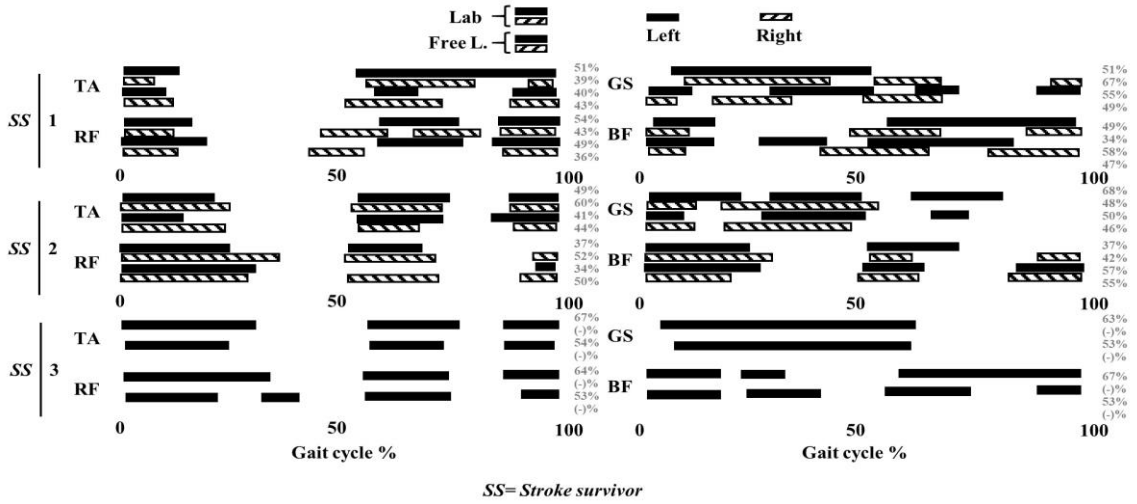

Figure 5. Muscle activity pattern stroke survivors for indoor vs. outdoor ground level walking. IC-FC moments were not able to detect for the paretic side of SS survivor (#3). Thus, only the left side muscle activity patterns are segmented only.

4.3. Impact of changing terrain

The fusion approach can quantify multi-model gait characteristics on different terrains, but we present level ground data only. Multi-model gait characteristics and descriptions of HP's and SS during different indoor (e.g., stairs) and outdoor (e.g., cobbles) terrains are presented in online supplementary material (Appendices A to D) but mentioned briefly here.

- Spatio-temporal characteristics: Comparing spatio-temporal gait characteristics of HP and SS in four domains during indoor/outdoor walking activities revealed notable differences. Among all indoor/outdoor walking activities of HP, the highest *pace* along with the lowest *rhythm* and *asymmetry* were found during outdoor level walking. Also, spatial parameters experienced the highest values for the *variability* domain, whereas temporal parameters were found second-highest in outdoor level walking after incline walking.
  SS groups experienced slightly increased *pace* and increased *asymmetry* during outdoor walking compared to indoor.
- Knee joint kinematics: HP revealed that mean knee flexion angles did not experience significant change while indoor/outdoor ground-level walking and walking on a rock surface.
  SS group revealed a slightly increased knee flexion angle (~4°) during outdoor level walking compared to indoor level walking. When comparing the paretic side and non-paretic side knee flexion angles of each SS, higher differences observed, Figure 4-c2.
- EMG, burst timing and durations during level walking: Prevalence of muscle burst and duration showed similar patterns between the right and left sides of lower limb muscles in most HP. Additionally, durations of muscle burst slightly decreased during outdoor level walking compared to indoor in most HP.
  The durations of muscle burst found slightly decreased during outdoor level walking compared to indoor in most SS.

5. Discussion

To the authors' knowledge, this is the first study to present and explores multi-modal sensor, algorithm and data fusion in clinic/lab and habitual/free-living gait. The methodologies provide a comprehensive range of lower limb gait characteristics (spatio-temporal, kinematics, and EMG) for use in different environments. The work presented here shows how algorithms developed in isolation can be successfully adapted and fused to create a more rounded/holistic gait assessment tool for use in the clinic/lab and beyond. The multi-modal fusion approach proposed here may better contribute to gait studies for clinical as well as habitual gait assessments, better informing rehabilitation programs that aim to regain community-based ambulatory mobility for those with neurological conditions such as stroke. Improved understanding of gait through our proposed multi-modal approach could lead to better understanding the effect of walking environment and how that contributes to the underlying mechanisms to reduce mobility and induce falls.

The proposed fusion methodology defined here consists of detection IC-FC contact moments along with timestamp information (using ***A1***-***A2*** algorithms and shank sensors data) by considering the type of activity (e.g., level walking or incline walking). That enables segmentation of gait cycles and sub-phases (stance and swing periods) as well as extraction of temporal parameters (e.g., step time). Then, gait cycles are segmented from mid-stance to mid-stance using the IC-FC information obtained from ***A1***-***A2***, and spatial characteristics (***A3*** and shank sensors data). Afterwards, knee joint flexion angles are estimated (***A4***-***A5*** and shank-thigh sensors data) by considering the type of activity (e.g., level walking or stair ambulation) for each gait cycle segmented. Finally, segmented gait cycles and corresponding timestamp information were used to segment EMG data belonging to four different lower limb muscles and muscle onset/offset timings (using ***A6***).

Previous studies have investigated gait during free-living to better understand the impacts of real-life settings such as environmental factors on gait [69, 70]. Most of these studies aim to extract clinically useful gait characteristics (spatio-temporal, kinematics) and are based on camera and IMUs. However, camera-based systems are not pragmatically feasible due to several factors such as privacy, security and, limited data capture due to field of vision [3, 71]. Although existing inertial sensor-based studies use a more feasible data collection approach, most fail to include clinically useful gait characteristics such as lower limb kinematics [72]. Additionally, the number of those focusing on free-living gait analysis in neurological conditions (e.g. stroke) is very limited and provides uni-modal characteristics only [3]. Those who investigated a multi-sensor fusion approach, utilised wearable sensors attached to the right lower limb for use during indoor level walking only [34]. Although that study quantified kinetic characteristics with a pressure sensor, spatial characteristics were not included.

5.1. The multi-modal approach

Multi-modal wearable sensor deployment is of growing interest during free-living activities. For instance, an approach to develop a vital sign monitoring system involving physiological components (e.g., respiratory band, electrocardiography) has been presented previously [53]. Another study used a similar approach where multiple

sensors were fused to develop a body sensor network that can measure motor functions in children with spastic diplegia [33]. Multi-modal wearable sensor use is possible due to the miniaturisation of wearable technologies and the increasing paradigm shift to monitoring people in their habitual environments. As gait is now classed as the sixth vital sign [73], it is important that multi-modal approaches are developed to capture gait in its entirety across more natural environments.

Most gait analysis studies have been conducted that do not immediately aim to make clinical decisions but to learn about a condition affecting a group of patients or the effect of an intervention [74]. Also, studies are based on a single sensor and provide either activity detection or informative gait outcomes. However, the next generation of wearables could be fused in a way that human activity assessment (i.e. activity detection and gait characteristics extraction) can be done using multiple sensor configurations [32]. Contemporary gait analysis requires evaluation of various aspects (e.g. kinematic, muscle) of the lower limb with a large number of outcomes [3]. Variances in gait are very subtle [45], and so the multi-modal gait approach enables granular capture of characteristics considering key digital biomarkers, i.e., clinically relevant gait characteristics. A study already reported that these variances/fluctuations in gait can be used to differentiate a particular neurological condition from healthy participants using gait data along with complexity measures [75]. Here, subtle differences were observed between indoor and outdoor level walking (as the differences between walking on various outdoor surfaces and stair ambulation) for HP and SS. This corroborates the benefit of using wearables for outdoor/habitual gait assessment as observed in another neurological cohort, albeit with a uni-modal device in Parkinson's disease [24]. Use of a multi-modal sensor and data fusion approach may provide more insights into the underlying neurological mechanisms due to, e.g., changing terrain.

Spatio-temporal outcomes have been widely used to reveal distinctive gait deficits and interpret impaired gait during indoor and outdoor assessments. Particularly for outdoor assessments, a previous study reported gait adaptations strategies to maintain stability are sensitive to different walking surfaces [50]. Thus, investigating the adaptation of *pace* on various surfaces may help better understand control on the sensory, motor and cortical functions that are critical to minimise trips, slips and falls [3]. Additionally, the proposed multi-modal sensor fusion approach efficiently computed spatio-temporal characteristics during indoor and outdoor gait for a more holistic gait assessment. Here, extracted spatio-temporal characteristics (e.g., indoor step, stance, swing times: 0.566s, 0.647s, 0.489s, respectively, outdoor step, stance, swing times: 0.534s, 0.597s, 0.476s, respectively) show good agreement with previous indoor level walking (0.534s, 0.668s, 0.401s) [76] and outdoor level walking (0.593s, 0.741s, 0.449s) studies [24] for HP. The small difference between the extracted temporal results perhaps is due to the difference between preferred experimental protocols, preferred sensor location, sensors, and algorithms. This is equally true for SS; indoor level walking (step, stance, swing times: 0.614s, 0.770s, 0.483s, respectively) and outdoor level walking (step, stance, swing times: 0.535s, 0.748s, 0.452s, respectively) findings of this study show good agreement with a previous study [51], where indoor level walking (step, stance, swing times: 0.6 s 0.743s 0.485, respectively) and outdoor level walking (step, stance, swing times: 0.613s, 0.764s, 0.474s) are reported. However, small differences (e.g., in stance-swing times <0.09s) were also observed in the stroke population due to referenced studies using a single IMU attached to the lower back compared to our approach of two IMU's attached to both shanks. Performance comparison of sensor locations and used methodology was further investigated[55, 56]. It was found that the shank-based methods provide more accurate temporal results compared to lower back based methods because the sensor is closer to IC-FC points of the foot. Moreover, reference studies used an algorithm based on acceleration signals whereas the proposed fusion approach used algorithms based on angular velocity for extracting spatiotemporal outcomes. The proposed multi-modal approach also attests to the existing knowledge that stroke survivors are high likely to experience decreased stance time and increased swing time in the paretic side, compared to non-paretic[77], Table S7.

Many physical therapy techniques focus on the restoration of joint kinematics and hence promote rehabilitation of functional activities [78]. Thus, kinematic joint characteristics are crucial as these characteristics provide additional insight into indoor/outdoor gait analysis. The prevalence of joint kinematic analysis in gait studies is low as kinematic characteristics require lab-based motion analysis systems that are complex and costly or goniometers, which brings synchronisation issue with other technologies [3]. Alternatively, a few gait studies estimate joint angles (e.g. knee flexion) during indoor and outdoor activities using wearable sensors [39, 41]. Findings of the proposed multi-modal sensor fusion tool (62.621°, 48.120° for indoor level walking of HP and SS, respectively) show good agreement with previous study findings based on indoor level walking (~60°, ~40° for indoor level walking of HP and SS) [79, 80] and outdoor [81, 82] activities in terms of estimated knee joint angles. Additionally, stroke participants experience decreased knee flexion angles during indoor/outdoor level walking in the paretic side, compared to non-paretic as previously reported [80].

Muscle activation pattern analysis of one or more muscles, particularly when the examination is conducted together with additional gait characteristics such as kinematics (joint angles), provides better insight into the performance of muscles and their role in accomplishing a motor task [43]. Although other crucial parameters, such as walking velocity and age that affect muscle burst timing and durations exist [83], comprehensive knowledge of

muscle activation and co-activation may contribute to the individualised bespoke rehabilitation programs[67]. The findings of the proposed multi-modal fusion tool attest to the common muscle activation patterns in terms of muscle burst timings and durations during indoor [83, 84] and outdoor activities [43, 85].

5.2. Implementation

Importantly, extraction of multi-model gait characteristics starts with the detection of gait cycles, IC and FC events. ***A1*** and ***A2*** were sufficient to estimate IC-FC moments during level walking (as well as incline walking and stair ambulation) for HP's and non-paretic sides of SS. However, failing to detect IC-FC events in the paretic side of SS, where significant foot clearance is lacking, negatively impacts the multi-model gait characteristics (primarily temporal) to be extracted. Alternatively, spatial characteristics successfully computed with ***A3*** for HP and non-paretic sides of SS, but similar problems occurred for the paretic sides of SS (section 5.3).

Sensor misplacement is also a consideration that needs to be considered during the implementation of this framework. It was previously reported that algorithms that use angular velocity for IC-FC detection (such as ***A1*** and ***A2***) are less sensitive to positioning compared to acceleration due to their measurement principle. ***A3*** and ***A5*** also stated that the sensor placement anywhere along the same plane on the anatomical segment (e.g., shank) gives almost identical signal output [11, 23, 40]. The proposed tool has potential use in free-living as it enables an extended period of data recording opportunities. Gyroscopes tend to consume up to several hundred milliamperes whereas accelerometers consume in the range of a few microamperes [11]. The use of additional hardware or sensing capabilities such as EMG can increase energy consumption significantly. Therefore, the energy consumption of the hardware (sensor) to be used should be taken into consideration. Here we use the Shimmer3 EMG sensor, which can be used in clinical studies as it provides reliable output for around 70 hours, depending on the activated sensing capabilities (e.g., sampling frequencies). Sensors that can collect data for a week or more are also available but there is a trade-off between e.g., data resolution, battery life and memory [3].

A review for sensor fusion use in orientation tracking found that advanced algorithms such as extended Kalman filter and complementary filter approaches should meet the need to perform offline calibration, vector selection technique for imperfect measurement rejection [86]. Although high accuracy and robust estimations were reported, these approaches are complex and require prior technical information regarding the IMUs to be used. Here, we proposed a less complex and more practical novel approach ***(A5)*** to estimate knee flexion angles during stair ambulation and incline walking by novel combination of two different validated algorithms [40, 42]. That approach allowed us to achieve a knee joint flexion angle approach that works during stair ambulation and without a need for prior configuration coefficients during orientation estimation.

EMG signals were segmented for each gait cycle using IC-FC timed events. Segmented raw EMG signals are difficult to interpret with a visual inspection alone [67]. Thus, processing raw EMG signals allow the extraction of clinically useful outcomes (e.g., muscle burst timing). Additionally, normalisation of EMG signals is crucial to make comparisons between muscles on different days or in different individuals during different walking tasks. Most studies time normalise EMG signal into gait cycles (%) or sub phases (stance %). However, the same standardisation is not common for amplitude normalisation. Peak activation level mean activation level, maximum voluntary contraction and peak to peak maximum amplitude (M wave) normalisation approaches have been widely used [67]. Although there are standards for EMG data collection (SENIAM), EMG signal processing standards are needed to achieve a more consistent EMG-based gait assessment [3].

5.3. Limitations and future work

Wearables offer high resolution data recording opportunities for extended periods. Continuous recording during free-living may result in a vast amount of unlabelled data that includes different daily dynamic gait activities (e.g. level walking, stair ambulation) and static activities (e.g. sitting, lying). Here, the proposed framework was used with manually segmented gait data (e.g., indoor level walking). However, manual segmentation of different activities before feeding into the proposed framework is a limitation to achieve a more automatic gait assessment tool. Therefore, automatic recognition of all activities (also known as human activity recognition, HAR) would provide a more pragmatic gait analysis tool, negating the time-consuming manual segmentation adopted here. Previous studies report that wearables can be deployed to recognise gait events with high accuracies using artificial intelligence approaches (e.g. machine learning, deep learning) [87, 88].

The time spent on sensor configuration and placement before data collection can be accepted as a limitation since it was approx. 50% of the total testing time for each participant. Here, the configuration of wearables and placement took 15-20 min for each participant. Much of the time (≈10 min) was spent on the placement of surface EMG electrodes and their connections with sensor units using wires. Technology is becoming more user friendly with wireless EMG sensors which could significantly decrease the setup time of wearables.

Successful implementation of the proposed multi-modal approach is significantly dependent on the correct detection of IC-FC times that is used to split gait into sub-phases and extract joint angles and muscle

activities. As presented in (Figure 4, b), more oscillations were observed in paretic side angular velocity compared to the non-paretic side of a stroke survivor. These oscillations affect the accuracy of proposed algorithms (e.g. ***A1***) as these algorithms estimate IC-FC times by taking reference to a single positive peak (mid-swing) [89]. In the paretic side of SS (#3), more oscillations were observed in peaks during mid-swing, and negative peaks were not present for the detection of IC-FC moments. Therefore, the proposed algorithms (***A1*** and ***A2***) failed to detect IC-FC moments, and consequently kinematic and muscle characteristics could not be extracted for the gait cycles.

Some algorithms presented here use a set of rules and thresholds. The use of threshold-based algorithms could be a limitation since time and frequency domain features of the wearable signals can be significantly affected by several factors such as weight, age, severity of impaired gait and walking speed. Alternatively, previous studies suggested that although amplitudes of these peaks vary depending on different factors, IC-FC moments can always be localised once approximate locations are known in time and frequency domains [3, 18]. Therefore, appropriate signal processing approaches (e.g. advanced wavelet) and artificial intelligent (machine learning, deep learning) approaches should be used in future studies to overcome this limitation [90]. Equally, developing new algorithms by considering signal power and statistical features rather than wave shape could be a solution for the algorithms that rely on peak detection.

5.3.1. Factors influencing accuracy of gait characteristics

Small errors and systematic delays (e.g. <0.009s) are present even in two different gold/reference standard system [55]. Therefore, it is crucial to investigate and interpret the agreement levels between reference systems and wearable sensors with caution. Although most inertial signal-based validation studies reported very good agreements when compared to a gold standard system[18, 39], the developed algorithms were validated on healthy participants only during controlled environments. When these algorithms were adopted to use in a neurological population, it was observed that their accuracies decrease [23, 54]. The primary reason for the poor performances of the algorithms is because movement patterns of hip and lower-limb segments experience different acceleration and angular velocity compared to healthy participants[54]. The secondary reason is the effects of the walking environments. This was further investigated by Storm *et al.* and reported that shank sensor-based algorithms such as ***A1***-***A2*** perform better in outdoor walking in terms of detecting some temporal parameters (e.g., stance time) compared to indoor walking [55]. The other reasons that affect the accuracy of inertial signal-based gait outcomes are preferred sensor locations (e.g., shank, lower back) and used target signal (e.g., acceleration, angular velocity) in the experimental protocol. A previous study investigated the impact of both factors on the extracted parameters, and findings showed that shank level sensor- angular velocity signals pair provide more accurate and repeatable results than lower back sensor- acceleration signal algorithms for healthy participants[38].

Our future work will aim to:

(i) investigate validity in a larger stroke cohort with the latest technology wearable sensors (e.g., wireless EMG),

(ii) integrate automated gait detection into a multi-modal fusion approach to achieve an automatic approach and,

(iii) investigate potential solutions for better detecting IC-FC moments in neurological conditions, particularly in severely disrupted gait.

6. Conclusion

This paper proposes a multi-modal gait assessment, enabling a comprehensive indoor and outdoor gait analysis using wearables. A multi-layered sensor, data and gait characteristic fusion approach was developed by utilising previously validated algorithms and adopting a robust methodological approach. The proposed fusion approach has a potential for utility in a more holistic gait analysis approach for use on various indoor and outdoor terrains. Detection of IC and FC events is key to ensure the utility of the fusion approach is fully realised, failure to detect those gait events may lead to missed gait characteristic. However, that may only be evident in the most impaired gait. Study findings show initial effectiveness of the approach by displaying the difference between indoor and outdoor experiments in spatio-temporal, knee joint kinematics and muscle activities, which could be informative for devising individualised rehabilitation strategies. Future work will investigate deployment on larger, more clinically well-defined SS and towards automated gait detection and segmentation.

References

[1] M. Roberts, D. Mongeon, F. Prince, Biomechanical parameters for gait analysis: a systematic review of healthy human gait, Phys Ther Rehabil, 4 (2017) 6.

[2] B. Balaban, F. Tok, Gait disturbances in patients with stroke, PM&R, 6 (2014) 635-642.

[3] Y. Celik, S. Stuart, W.L. Woo, A. Godfrey, Gait analysis in neurological populations: Progression in the use of wearables, Medical Engineering & Physics, (2020).

[4] S.L. James, L.R. Lucchesi, C. Bisignano, C.D. Castle, Z.V. Dingels, J.T. Fox, E.B. Hamilton, N.J. Henry, K.J. Krohn, Z. Liu, The global burden of falls: global, regional and national estimates of morbidity and mortality from the Global Burden of Disease Study 2017, Injury prevention, 26 (2020) i3-i11.
[5] J. Verghese, A.F. Ambrose, R.B. Lipton, C. Wang, Neurological gait abnormalities and risk of falls in older adults, Journal of neurology, 257 (2010) 392-398.
[6] J. Chen, K. Kwong, D. Chang, J. Luk, R. Bajcsy, Wearable sensors for reliable fall detection, in: 2005 IEEE Engineering in Medicine and Biology 27th Annual Conference, IEEE, 2006, pp. 3551-3554.
[7] C. Buckley, L. Alcock, R. McArdle, R.Z.U. Rehman, S. Del Din, C. Mazzà, A.J. Yarnall, L. Rochester, The role of movement analysis in diagnosing and monitoring neurodegenerative conditions: Insights from gait and postural control, Brain sciences, 9 (2019) 34.
[8] C.L. Richards, S.J. Olney, Hemiparetic gait following stroke. Part II: Recovery and physical therapy, Gait & posture, 4 (1996) 149-162.
[9] A. Cereatti, D. Trojaniello, U. Della Croce, Accurately measuring human movement using magneto-inertial sensors: techniques and challenges, in: 2015 IEEE International Symposium on Inertial Sensors and Systems (ISISS) Proceedings, IEEE, 2015, pp. 1-4.
[10] S. Díaz, J.B. Stephenson, M.A. Labrador, Use of wearable sensor technology in gait, balance, and range of motion analysis, Applied Sciences, 10 (2020) 234.
[11] J. Rueterbories, E.G. Spaich, B. Larsen, O.K. Andersen, Methods for gait event detection and analysis in ambulatory systems, Medical engineering & physics, 32 (2010) 545-552.
[12] F. Demrozi, G. Pravadelli, A. Bihorac, P. Rashidi, Human activity recognition using inertial, physiological and environmental sensors: a comprehensive survey, IEEE Access, (2020).
[13] P. Ortega-Bastidas, P. Aqueveque, B. Gómez, F. Saavedra, R. Cano-de-la-Cuerda, Use of a Single Wireless IMU for the Segmentation and Automatic Analysis of Activities Performed in the 3-m Timed Up & Go Test, Sensors, 19 (2019) 1647.
[14] Y. Celik, D. Powell, W.L. Woo, S. Stuart, A. Godfrey, A feasibility study towards instrumentation of the Sport Concussion Assessment Tool (iSCAT), in: 2020 42nd Annual International Conference of the IEEE Engineering in Medicine & Biology Society (EMBC), IEEE, 2020, pp. 4624-4627.
[15] B. Sijobert, J. Denys, C.A. Coste, C. Geny, IMU based detection of freezing of gait and festination in Parkinson's disease, in: 2014 IEEE 19th International Functional Electrical Stimulation Society Annual Conference (IFESS), IEEE, 2014, pp. 1-3.
[16] A. Behboodi, N. Zahradka, H. Wright, J. Alesi, S. Lee, Real-time detection of seven phases of gait in children with cerebral palsy using two gyroscopes, Sensors, 19 (2019) 2517.
[17] R. Mc Ardle, S. Del Din, B. Galna, A. Thomas, L. Rochester, Differentiating dementia disease subtypes with gait analysis: feasibility of wearable sensors?, Gait & Posture, 76 (2020) 372-376.
[18] K. Aminian, B. Najafi, C. Büla, P.-F. Leyvraz, P. Robert, Spatio-temporal parameters of gait measured by an ambulatory system using miniature gyroscopes, Journal of biomechanics, 35 (2002) 689-699.
[19] J. McCamley, M. Donati, E. Grimpampi, C. Mazza, An enhanced estimate of initial contact and final contact instants of time using lower trunk inertial sensor data, Gait & posture, 36 (2012) 316-318.
[20] P. Catalfamo, S. Ghoussayni, D. Ewins, Gait event detection on level ground and incline walking using a rate gyroscope, Sensors, 10 (2010) 5683-5702.
[21] P.C. Formento, R. Acevedo, S. Ghoussayni, D. Ewins, Gait event detection during stair walking using a rate gyroscope, Sensors, 14 (2014) 5470-5485.
[22] E. Bishop, Q. Li, Walking speed estimation using shank-mounted accelerometers, in: 2010 IEEE International Conference on Robotics and Automation, IEEE, 2010, pp. 5096-5101.
[23] B. Sijobert, M. Benoussaad, J. Denys, R. Pissard-Gibollet, C. Geny, C.A. Coste, Implementation and validation of a stride length estimation algorithm, using a single basic inertial sensor on healthy subjects and patients suffering from Parkinson's disease, ElectronicHealthcare, (2015) 704-714.
[24] S. Del Din, A. Godfrey, B. Galna, S. Lord, L. Rochester, Free-living gait characteristics in ageing and Parkinson’s disease: impact of environment and ambulatory bout length, Journal of neuroengineering and rehabilitation, 13 (2016) 46.
[25] A. Weiss, S. Sharifi, M. Plotnik, J.P. van Vugt, N. Giladi, J.M. Hausdorff, Toward automated, at-home assessment of mobility among patients with Parkinson disease, using a body-worn accelerometer, Neurorehabilitation and neural repair, 25 (2011) 810-818.
[26] N. Hatanaka, K. Sato, N. Hishikawa, M. Takemoto, Y. Ohta, T. Yamashita, K. Abe, Comparative gait analysis in progressive supranuclear palsy and Parkinson's disease, European neurology, 75 (2016) 282-289.
[27] G. Chen, C. Patten, D.H. Kothari, F.E. Zajac, Gait differences between individuals with post-stroke hemiparesis and non-disabled controls at matched speeds, Gait & posture, 22 (2005) 51-56.
[28] S. Nadeau, M. Betschart, F. Bethoux, Gait analysis for poststroke rehabilitation: the relevance of biomechanical analysis and the impact of gait speed, Physical Medicine and Rehabilitation Clinics, 24 (2013) 265-276.

[29] R. Morris, A. Hickey, S. Del Din, A. Godfrey, S. Lord, L. Rochester, A model of free-living gait: a factor analysis in Parkinson's disease, Gait & posture, 52 (2017) 68-71.
[30] S. Stuart, L. Parrington, R. Morris, D.N. Martini, P.C. Fino, L.A. King, Gait measurement in chronic mild traumatic brain injury: A model approach, Human movement science, 69 (2020) 102557.
[31] T. Lencioni, I. Carpinella, M. Rabuffetti, A. Marzegan, M. Ferrarin, Human kinematic, kinetic and EMG data during different walking and stair ascending and descending tasks, Scientific data, 6 (2019) 1-10.
[32] M. Seiffert, F. Holstein, R. Schlosser, J. Schiller, Next generation cooperative wearables: Generalized activity assessment computed fully distributed within a wireless body area network, IEEE Access, 5 (2017) 16793-16807.
[33] J. Li, Z. Wang, S. Qiu, H. Zhao, Q. Wang, D. Plettemeier, B. Liang, X. Shi, Using Body Sensor Network to Measure the Effect of Rehabilitation Therapy on Improvement of Lower Limb Motor Function in Children With Spastic Diplegia, IEEE Transactions on Instrumentation and Measurement, 69 (2020) 9215-9227.
[34] C. Cruz-Montecinos, S. Pérez-Alenda, F. Querol, M. Cerda, H. Maas, Changes in muscle activity patterns and joint kinematics during gait in hemophilic arthropathy, Frontiers in physiology, 10 (2020) 1575.
[35] S. Chung, J. Lim, K.J. Noh, G. Kim, H. Jeong, Sensor data acquisition and multimodal sensor fusion for human activity recognition using deep learning, Sensors, 19 (2019) 1716.
[36] H. Zhao, Z. Wang, S. Qiu, J. Wang, F. Xu, Z. Wang, Y. Shen, Adaptive gait detection based on foot-mounted inertial sensors and multi-sensor fusion, Information Fusion, 52 (2019) 157-166.
[37] J. Wang, Z. Wang, S. Qiu, J. Xu, H. Zhao, G. Fortino, M. Habib, A selection framework of sensor combination feature subset for human motion phase segmentation, Information Fusion, (2020).
[38] G.P. Panebianco, M.C. Bisi, R. Stagni, S. Fantozzi, Analysis of the performance of 17 algorithms from a systematic review: Influence of sensor position, analysed variable and computational approach in gait timing estimation from IMU measurements, Gait & posture, 66 (2018) 76-82.
[39] R. Takeda, S. Tadano, A. Natorigawa, M. Todoh, S. Yoshinari, Gait posture estimation using wearable acceleration and gyro sensors, Journal of biomechanics, 42 (2009) 2486-2494.
[40] K. Tong, M.H. Granat, A practical gait analysis system using gyroscopes, Medical engineering & physics, 21 (1999) 87-94.
[41] H. Dejnabadi, B.M. Jolles, K. Aminian, A new approach to accurate measurement of uniaxial joint angles based on a combination of accelerometers and gyroscopes, IEEE Transactions on Biomedical Engineering, 52 (2005) 1478-1484.
[42] L.F. Nestares, R. Callupe, Development of a wearable motion capture system to evaluate the knee joint angle during stair-climbing in hemiplegics, in: 2020 IEEE XXVII International Conference on Electronics, Electrical Engineering and Computing (INTERCON), IEEE, 2020, pp. 1-4.
[43] M.G. Benedetti, V. Agostini, M. Knaflitz, P. Bonato, Muscle activation patterns during level walking and stair ambulation, Applications of EMG in clinical and sports medicine, 8 (2012) 117-130.
[44] A. Den Otter, A. Geurts, T. Mulder, J. Duysens, Gait recovery is not associated with changes in the temporal patterning of muscle activity during treadmill walking in patients with post-stroke hemiparesis, Clinical Neurophysiology, 117 (2006) 4-15.
[45] A. Zhao, J. Li, J. Dong, L. Qi, Q. Zhang, N. Li, X. Wang, H. Zhou, Multimodal Gait Recognition for Neurodegenerative Diseases, arXiv preprint arXiv:2101.02469, (2021).
[46] H.F. Nweke, Y.W. Teh, G. Mujtaba, M.A. Al-Garadi, Data fusion and multiple classifier systems for human activity detection and health monitoring: Review and open research directions, Information Fusion, 46 (2019) 147-170.
[47] S. Qiu, L. Liu, H. Zhao, Z. Wang, Y. Jiang, MEMS inertial sensors based gait analysis for rehabilitation assessment via multi-sensor fusion, Micromachines, 9 (2018) 442.
[48] C.-W. Lin, Y.-T.C. Yang, J.-S. Wang, Y.-C. Yang, A wearable sensor module with a neural-network-based activity classification algorithm for daily energy expenditure estimation, IEEE Transactions on Information Technology in Biomedicine, 16 (2012) 991-998.
[49] S.H. Roy, M.S. Cheng, S.-S. Chang, J. Moore, G. De Luca, S.H. Nawab, C.J. De Luca, A combined sEMG and accelerometer system for monitoring functional activity in stroke, IEEE Transactions on Neural Systems and Rehabilitation Engineering, 17 (2009) 585-594.
[50] K. Zurales, T.K. DeMott, H. Kim, L. Allet, J.A. Ashton-Miller, J.K. Richardson, Gait efficiency on an uneven surface is associated with falls and injury in older subjects with a spectrum of lower limb neuromuscular function: a prospective study, American journal of physical medicine & rehabilitation/Association of Academic Physiatrists, 95 (2016) 83.
[51] S.A. Moore, A. Hickey, S. Lord, S. Del Din, A. Godfrey, L. Rochester, Comprehensive measurement of stroke gait characteristics with a single accelerometer in the laboratory and community: a feasibility, validity and reliability study, Journal of neuroengineering and rehabilitation, 14 (2017) 130.
[52] S. Del Din, A. Godfrey, B. Galna, S. Lord, L. Rochester, Free-living gait characteristics in ageing and Parkinson's disease: impact of environment and ambulatory bout length, Journal of neuroengineering and

rehabilitation, 13 (2016) 1-12.
[53] E. Sejdić, A. Millecamps, J. Teoli, M.A. Rothfuss, N.G. Franconi, S. Perera, A. Jones, J.S. Brach, M.H. Mickle, Assessing interactions among multiple physiological systems during walking outside a laboratory: An android based gait monitor, Computer methods and programs in biomedicine, 122 (2015) 450-461.
[54] D. Trojaniello, A. Ravaschio, J.M. Hausdorff, A. Cereatti, Comparative assessment of different methods for the estimation of gait temporal parameters using a single inertial sensor: application to elderly, post-stroke, Parkinson's disease and Huntington's disease subjects, Gait & posture, 42 (2015) 310-316.
[55] F.A. Storm, C.J. Buckley, C. Mazzà, Gait event detection in laboratory and real life settings: Accuracy of ankle and waist sensor based methods, Gait & posture, 50 (2016) 42-46.
[56] K.B. Mansour, N. Rezzoug, P. Gorce, Analysis of several methods and inertial sensors locations to assess gait parameters in able-bodied subjects, Gait & posture, 42 (2015) 409-414.
[57] K.S. van Schooten, M. Pijnappels, S.M. Rispens, P.J. Elders, P. Lips, J.H. van Dieën, Ambulatory fall-risk assessment: amount and quality of daily-life gait predict falls in older adults, Journals of Gerontology Series A: Biomedical Sciences and Medical Sciences, 70 (2015) 608-615.
[58] A. Millecamps, K.A. Lowry, J.S. Brach, S. Perera, M.S. Redfern, E. Sejdić, Understanding the effects of pre-processing on extracted signal features from gait accelerometry signals, Computers in biology and medicine, 62 (2015) 164-174.
[59] A. Khan, N. Hammerla, S. Mellor, T. Plötz, Optimising sampling rates for accelerometer-based human activity recognition, Pattern Recognition Letters, 73 (2016) 33-40.
[60] K. Aminian, P. Robert, E. Jéquier, Y. Schutz, Incline, speed, and distance assessment during unconstrained walking, Medicine and science in sports and exercise, 27 (1995) 226-234.
[61] M.J. Mathie, A.C. Coster, N.H. Lovell, B.G. Celler, Accelerometry: providing an integrated, practical method for long-term, ambulatory monitoring of human movement, Physiological measurement, 25 (2004) R1.
[62] A. Findlow, J. Goulermas, C. Nester, D. Howard, L. Kenney, Predicting lower limb joint kinematics using wearable motion sensors, Gait & posture, 28 (2008) 120-126.
[63] M. Brodie, A. Walmsley, W. Page, The static accuracy and calibration of inertial measurement units for 3D orientation, (2008).
[64] C. Yi, J. Ma, H. Guo, J. Han, H. Gao, F. Jiang, C. Yang, Estimating three-dimensional body orientation based on an improved complementary filter for human motion tracking, Sensors, 18 (2018) 3765.
[65] R.E. Singh, K. Iqbal, G. White, J.K. Holtz, A Review of EMG Techniques for Detection of Gait Disorders, in: Machine Learning in Medicine and Biology, IntechOpen, 2019.
[66] J. Perry, The contribution of dynamic electromyography to gait analysis, J Rehabil Res Dev, 33 (1998).
[67] M. Halaki, K. Ginn, Normalization of EMG signals: to normalize or not to normalize and what to normalize to, Computational intelligence in electromyography analysis-a perspective on current applications and future challenges, (2012) 175-194.
[68] S. Srivastava, C. Patten, S.A. Kautz, Altered muscle activation patterns (AMAP): an analytical tool to compare muscle activity patterns of hemiparetic gait with a normative profile, Journal of neuroengineering and rehabilitation, 16 (2019) 21.
[69] P. DasMahapatra, E. Chiauzzi, R. Bhalerao, J. Rhodes, Free-living physical activity monitoring in adult US patients with multiple sclerosis using a consumer wearable device, Digital Biomarkers, 2 (2018) 47-63.
[70] E.E. Stone, M. Skubic, Capturing habitual, in-home gait parameter trends using an inexpensive depth camera, in: 2012 Annual International Conference of the IEEE Engineering in Medicine and Biology Society, IEEE, 2012, pp. 5106-5109.
[71] G. Demiris, D.P. Oliver, J. Giger, M. Skubic, M. Rantz, Older adults' privacy considerations for vision based recognition methods of eldercare applications, Technology and Health Care, 17 (2009) 41-48.
[72] F. Deligianni, C. Wong, B. Lo, G.-Z. Yang, A fusion framework to estimate plantar ground force distributions and ankle dynamics, Information Fusion, 41 (2018) 255-263.
[73] A. Middleton, S.L. Fritz, M. Lusardi, Walking speed: the functional vital sign, Journal of aging and physical activity, 23 (2015) 314-322.
[74] R. Baker, Gait analysis methods in rehabilitation, Journal of neuroengineering and rehabilitation, 3 (2006) 1-10.
[75] S. Lahmiri, Gait nonlinear patterns related to Parkinson's disease and age, IEEE Transactions on Instrumentation and Measurement, 68 (2018) 2545-2551.
[76] A. Godfrey, S. Del Din, G. Barry, J. Mathers, L. Rochester, Instrumenting gait with an accelerometer: a system and algorithm examination, Medical engineering & physics, 37 (2015) 400-407.
[77] Y. Wang, M. Mukaino, K. Ohtsuka, Y. Otaka, H. Tanikawa, F. Matsuda, K. Tsuchiyama, J. Yamada, E. Saitoh, Gait characteristics of post-stroke hemiparetic patients with different walking speeds, International journal of rehabilitation research. Internationale Zeitschrift fur Rehabilitationsforschung. Revue internationale de recherches de readaptation, 43 (2020) 69.
[78] P. Rowe, C. Myles, C. Walker, R. Nutton, Knee joint kinematics in gait and other functional activities

measured using flexible electrogoniometry: how much knee motion is sufficient for normal daily life?, Gait & posture, 12 (2000) 143-155.
[79] J. Boudarham, N. Roche, D. Pradon, C. Bonnyaud, D. Bensmail, R. Zory, Variations in kinematics during clinical gait analysis in stroke patients, PloS one, 8 (2013).
[80] C. Bonnyaud, D. Pradon, N. Vuillerme, D. Bensmail, N. Roche, Spatiotemporal and kinematic parameters relating to oriented gait and turn performance in patients with chronic stroke, PloS one, 10 (2015).
[81] R. Riener, M. Rabuffetti, C. Frigo, Stair ascent and descent at different inclinations, Gait & posture, 15 (2002) 32-44.
[82] S. Vallabhajosula, C.W. Tan, M. Mukherjee, A.J. Davidson, N. Stergiou, Biomechanical analyses of stair-climbing while dual-tasking, Journal of biomechanics, 48 (2015) 921-929.
[83] A. Schmitz, A. Silder, B. Heiderscheit, J. Mahoney, D.G. Thelen, Differences in lower-extremity muscular activation during walking between healthy older and young adults, Journal of electromyography and kinesiology, 19 (2009) 1085-1091.
[84] A. Den Otter, A. Geurts, T. Mulder, J. Duysens, Abnormalities in the temporal patterning of lower extremity muscle activity in hemiparetic gait, Gait & posture, 25 (2007) 342-352.
[85] H. Yali, S. Aiguo, G. Haitao, Z. Songqing, The muscle activation patterns of lower limb during stair climbing at different backpack load, Acta of Bioengineering and Biomechanics, 17 (2015).
[86] M. Nazarahari, H. Rouhani, 40 years of sensor fusion for orientation tracking via magnetic and inertial measurement units: Methods, lessons learned, and future challenges, Information Fusion, 68 (2021) 67-84.
[87] A. Kececi, A. Yildirak, K. Ozyazici, G. Ayluctarhan, O. Agbulut, I. Zincir, Implementation of machine learning algorithms for gait recognition, Engineering Science and Technology, an International Journal, 23 (2020) 931-937.
[88] O.M. Giggins, I. Clay, L. Walsh, Physical activity monitoring in patients with neurological disorders: a review of novel body-worn devices, Digital Biomarkers, 1 (2017) 14-42.
[89] S. Yang, J.-T. Zhang, A.C. Novak, B. Brouwer, Q. Li, Estimation of spatio-temporal parameters for post-stroke hemiparetic gait using inertial sensors, Gait & posture, 37 (2013) 354-358.
[90] M. Gadaleta, G. Cisotto, M. Rossi, R.Z.U. Rehman, L. Rochester, S. Del Din, Deep learning techniques for improving digital gait segmentation, in: 2019 41st Annual International Conference of the IEEE Engineering in Medicine and Biology Society (EMBC), IEEE, 2019, pp. 1834-1837.

ONLINE SUPPLEMENTARY MATERIAL: APPENDICES

A. Impact of changing terrain

Walking on uneven rock surface and inclined walking were excluded for stroke survivors due to safety reasons. The environments' and cohorts information for extracted parameters for the purpose of this study are presented in Table S1.

Table A1 Extracted parameters in environments/activities for healthy participants (HP) and stroke survivors (SS) for the purpose of the study

Environment/activity	Cohort	Spatio-temporal	Knee joint angle	Muscle activity
Indoor level walking	*HP-SS*	✓	✓	✓
Outdoor level walking	*HP-SS*	✓	✓	✓
Incline walking	*HP only*	✓	✓	*X*
Walking on rock surface	*HP only*	✓	✓	*X*
Stair ascent/descent	*HP-SS*	*X*	✓	✓

B. Spatio-temporal outcomes

HP: Small but substantial impacts of changing terrain observed in four gait domains, Table S1. Comparing spatio-temporal characteristics of outdoor activities revealed that variability is highest in temporal characteristics during incline walking (ascent slope) compared to other activities. Additionally, higher variability observed in level walking compared to walking on a rock surface and the differences in variability found higher in spatial parameters compared to temporal. HP walks with decreased *rhythm* and increased *pace*, *variability* and *asymmetry* during incline walking compared to walking on a rock surface.

Table B1 Spatio-temporal gait characteristics of HP ground level walking in indoor and outdoor, 2min

	Indoor									
	1	**2**	**3**	**4**	**5**	**6**	**7**	**8**	**9**	**10**
# of strides	*104*	*105*	*103*	*76*	*95*	*104*	*124*	*103*	*100*	*82*
PACE										
Mean Stride V. (m/s)	1.361	1.11	1.291	0.943	1.204	1.27	1.273	1.205	1.077	1.015
Mean Stride L. (m)	1.569	1.242	1.493	1.073	1.406	1.438	1.161	1.349	1.371	1.223
RHYTHM										
Mean Stride Time (s)	1.150	1.118	1.158	1.134	1.165	1.131	0.912	1.117	1.270	1.206
Mean Step Time (s)	0.576	0.560	0.579	-	0.594	0.566	0.468	0.559	0.590	0.604
Mean Stance Time (s)	0.699	0.616	0.65	0.638	0.639	0.635	0.510	0.653	0.719	0.715
Mean Swing Time (s)	0.45	0.502	0.508	0.496	0.526	0.497	0.402	0.465	0.554	0.491
VARIABILITY										
Stride V. Var (m/s)	0.143	0.085	0.133	0.099	0.111	0.074	0.077	0.085	0.106	0.142
Stride L Var (m)	0.171	0.103	0.161	0.122	0.149	0.085	0.063	0.088	0.175	0.186
Step Time Var (s)	0.005	0.007	0.059	-	0.038	0.031	0.033	0.019	0.071	0.043
Stance Time Var (s)	0.005	0.002	0.022	0.027	0.007	0.005	0.008	0.022	0.033	0.011
Swing Time Var (s)	0.008	0.005	0.02	0.013	0.039	0.006	0.036	0.022	0.025	0.007
ASYMMETRY										
Stride L. Asy (m)	0.050	0.015	0.139	0.065	0.088	0.181	0.125	0.004	0.177	0.019
Step Time Asy (s)	0.029	0.039	0.044	-	0.037	0.026	0.027	0.027	0.043	0.032
Stance Time Asy (s)	0.037	0.034	0.043	0.062	0.057	0.03	0.042	0.03	0.036	0.039
Swing Time Asy (s)	0.041	0.048	0.048	0.043	0.059	0.039	0.036	0.034	0.053	0.045
	Outdoor									
	1	**2**	**3**	**4**	**5**	**6**	**7**	**8**	**9**	**10**
# of strides	*98*	*114*	*108*	*118*	*103*	*108*	*120*	*96*	*100*	*116*
PACE										
Mean Stride V. (m/s)	1.477	1.241	1.343	1.123	1.257	1.352	1.371	1.39	1.419	1.218
Mean Stride L. (m)	1.606	1.339	1.488	1.131	1.414	1.461	1.259	1.449	1.627	1.377
RHYTHM										
Mean Stride Time (s)	1.092	1.078	1.112	1.015	1.133	1.086	0.924	1.042	1.142	1.125
Mean Step Time (s)	0.547	0.546	0.556	0.499	0.567	0.545	0.464	0.521	-	0.566
Mean Stance Time (s)	0.648	0.589	0.622	0.557	0.6	0.604	0.51	0.588	0.622	0.636
Mean Swing Time (s)	0.444	0.489	0.490	0.452	0.533	0.481	0.413	0.455	0.519	0.488
VARIABILITY										
Stride V. Var (m/s)	0.160	0.124	0.109	0.124	0.116	0.08	0.141	0.112	-	0.159
Stride L Var (m)	0.173	0.13	0.119	0.125	0.134	0.11	0.086	0.106	-	0.185
Step Time Var (s)	0.035	0.033	0.035	0.049	0.035	0.041	0.036	0.02	-	0.071
Stance Time Var (s)	0.044	0.046	0.048	0.043	0.069	0.047	0.049	0.034	-	0.075
Swing Time Var (s)	0.043	0.043	0.044	0.042	0.051	0.046	0.042	0.034	-	0.044
ASYMMETRY										
Stride L. Asy (m)	0.126	0.143	0.125	0.019	0.057	0.248	0.024	0.056	-	0.138
Step Time Asy (s)	0.029	0.005	0.077	0.019	0.005	0.031	0.01	0.006	-	0.047
Stance Time Asy (s)	0.013	0.019	0.033	0.005	0.011	0.008	0.006	0.012	-	0.006
Swing Time Asy (s)	0.010	0.006	0.031	0.009	0.009	0.009	0.011	0.012	-	0.003

Table B2 Spatio-temporal gait characteristics of HPs during incline walking and walking on rock surface

	Incline walking										
	1	**2**	**3**	**4**	**5**	**6**	**7**	**8**	**9**	**10**	
# of strides	*8*	*9*	*11*	*10*	*7*	*7*	*7*	*8*	*7*	*7*	
PACE											**Average**
Mean Stride V. (m/s)	1.178	1.076	1.233	1.178	1.185	1.136	1.357	1.222	1.231	1.390	1.218
Mean Stride L. (m)	1.215	1.290	1.480	1.215	1.424	1.375	1.275	1.427	1.555	1.715	1.397
RHYTHM											
Mean Stride Time (s)	1.248	1.184	1.200	1.046	1.205	1.197	0.953	1.134	1.25	1.205	1.162
Mean Step Time (s)	0.619	0.608	0.606	0.555	0.617	0.597	0.477	0.565	-	0.625	0.585
Mean Stance Time (s)	0.693	0.652	0.64	0.578	0.683	0.684	0.529	0.614	0.706	0.709	0.648
Mean Swing Time (s)	0.555	0.531	0.556	0.469	0.523	0.513	0.424	0.521	0.547	0.496	0.513
VARIABILITY											
Stride V. Var (m/s)	0.085	0.068	0.059	0.085	0.180	0.124	0.183	0.136	-	0.124	0.113
Stride L Var (m)	0.091	0.094	0.046	0.091	0.208	0.158	0.116	0.141	-	0.149	0.120
Step Time Var (s)	0.048	0.037	0.057	0.057	0.398	0.037	0.036	0.062	-	0.024	0.084
Stance Time Var (s)	0.050	0.047	0.073	0.045	0.058	0.046	0.029	0.106	-	0.074	0.058
Swing Time Var (s)	0.060	0.065	0.076	0.050	0.056	0.050	0.048	0.066	-	0.035	0.057
ASYMMETRY											
Stride L. Asy (m)	0.030	0.21	0.259	0.030	0.046	0.437	0.030	0.366	-	0.020	0.158
Step Time Asy (s)	0.000	0.025	0.051	0.029	0.269	0.047	0.004	0.002	-	0.029	0.050
Stance Time Asy (s)	0.009	0.055	0.024	0.035	0.049	0.036	0.002	0.007	-	0.049	0.029
Swing Time Asy (s)	0.010	0.007	0.010	0.017	0.022	0.048	0.015	0.015	-	0.068	0.023
	Rock surface										
	1	**2**	**3**	**4**	**5**	**6**	**7**	**8**	**9**	**10**	
# of strides	*6*	*6*	*8*	*3*	*6*	*6*	*5*	*4*	*8*	*7*	
PACE											**Average**
Mean Stride V. (m/s)	1.126	1.137	1.066	1.126	1.129	1.196	1.289	1.372	1.356	1.241	1.203
Mean Stride L. (m)	1.21	1.364	1.315	1.21	1.466	1.507	1.319	1.589	1.582	1.515	1.407
RHYTHM											
Mean Stride Time (s)	1.096	1.172	1.239	1.096	1.346	1.283	1.063	1.149	1.161	1.229	1.183
Mean Step Time (s)	0.554	0.592	0.623	0.554	0.673	0.635	0.531	0.569	-	0.623	0.594
Mean Stance Time (s)	0.607	0.64	0.717	0.607	0.775	0.734	0.585	0.641	0.652	0.705	0.666
Mean Swing Time (s)	0.489	0.532	0.522	0.489	0.571	0.549	0.478	0.508	0.509	0.524	0.517
VARIABILITY											
Stride V. Var (m/s)	0.107	0.099	0.096	0.107	0.082	0.050	0.100	0.064	-	0.101	0.084
Stride L Var (m)	0.112	0.15	0.123	0.112	0.094	0.067	0.109	0.123	-	0.136	0.108
Step Time Var (s)	0.022	0.027	0.062	0.022	0.045	0.045	0.034	0.020	-	0.054	0.036
Stance Time Var (s)	0.057	0.066	0.061	0.057	0.049	0.042	0.037	0.039	-	0.075	0.052
Swing Time Var (s)	0.033	0.033	0.033	0.033	0.059	0.037	0.063	0.046	-	0.038	0.040
ASYMMETRY											
Stride L. Asy (m)	0.211	0.190	0.032	0.211	0.167	0.307	0.100	0.006	-	0.124	0.149
Step Time Asy (s)	0.007	0.040	0.068	0.007	0.016	0.022	0.005	0.013	-	0.031	0.023
Stance Time Asy (s)	0.006	0.033	0.004	0.006	0.027	0.022	0.001	0.008	-	0.011	0.013
Swing Time Asy (s)	0.019	0.028	0.038	0.019	0.000	0.009	0.003	0.013	-	0.02	0.016

(-) parameter not available due to data collection or synchronisation error,
Stride V = stride velocity, Stride L = stride length. Var = variability, Asy = asymmetry

Table B3 Spatio-temporal gait characteristics of SS ground level walking in indoor and outdoor

	Indoor			***Outdoor***		
	1	**2**	**3 [np]**	**1**	**2**	**3 [np]**
# of strides	*80*	*110*	*91*	*95*	*125*	*108*
PACE						
Mean Stride V. (m/s)	0.997	0.977	1.09	1.014	0.955	1.233
Mean Stride L. (m)	1.35	1.121	1.44	1.248	1.055	1.850
RHYTHM						
Mean Stride Time (s)	1.308	1.145	1.310	1.248	1.070	1.388
Mean Step Time (s)	0.656	0.573	-	0.547	0.524	-
Mean Stance Time (s)	0.766	0.668	0.878	0.669	0.627	0.948
Mean Swing Time (s)	0.542	0.477	0.432	0.476	0.443	0.439
VARIABILITY						
Stride V. Var (m/s)	0.203	0.176	-	0.216	0.149	-
Stride L Var (m)	0.322	0.229	-	0.277	0.172	-
Step Time Var (s)	0.196	0.004	-	0.027	0.040	-
Stance Time Var (s)	0.129	0.012	-	0.072	0.077	-
Swing Time Var (s)	0.123	0.019	-	0.035	0.040	-
ASYMMETRY						
Stride L. Asy (m)	0.018	0.376	-	0.108	0.473	-
Step Time Asy (s)	0.063	0.057	-	0.164	0.041	-
Stance Time Asy (s)	0.064	0.063	-	0.134	0.042	-
Swing Time Asy (s)	0.062	0.062	-	0.103	0.031	-

(-) parameter not available due to data collection or synchronisation error, Stride V = stride velocity, Stride L = stride length. Var = variability, Asy = asymmetry,(np) non paretic side only due to failing to detect IC-FC times

C. Knee joint kinematics

Knee joint kinematics (HP): Increased asymmetry in knee flexion angles while walking on a rock surface was notable compared to indoor/outdoor ground-level walking. During incline walking (ascent slope), HP experienced lower mean knee flexion angles compared to indoor/outdoor ground-level walking. Increased variance and asymmetry in knee flexion angles during incline walking were other findings compared to indoor/outdoor ground-level walking. Additionally, increased mean knee flexion angles and asymmetry were found to be common during walking on rock surfaces compared to incline walking

In the stair ambulation experiment, knee flexion angles found higher during stair descent compared to stair ascent. No significant differences observed in the asymmetry of knee flexion angles.

Knee joint kinematics (SS): Increased variability and asymmetry in knee flexion angles were observed during indoor level walking compared to outdoor level walking. Similarly, SS experienced higher knee flexion angles during stair ascent compared to stair descent. Additionally, increased variance and decreased asymmetry were present during stair descent compared to the ascent.

Table C1 Kinematic knee joint angles (degree) of HPs

Indoor level walking											
	1	**2**	**3**	**4**	**5**	**6**	**7**	**8**	**9**	**10**	
# of strides	*104*	*105*	*103*	*76*	*95*	*104*	*124*	*103*	*100*	*82*	
											Average
Mean	62.976	51.839	63.419	62.701	59.281	64.467	62.791	66.774	64.056	67.906	62.621
Var	5.328	4.818	4.025	7.706	4.028	4.321	4.693	4.438	7.202	5.316	5.1875
Asy	3.485	3.467	1.950	0.880	0.760	2.869	1.635	0.687	0.954	1.430	1.8117
Outdoor level walking											
# of strides	*98*	*114*	*108*	*118*	*103*	*108*	*120*	*96*	*100*	*116*	
											Average
Mean	63.819	51.529	63.577	64.202	56.731	65.022	65.256	67.821	69.000	68.839	63.5796
Var	4.746	5.103	3.043	6.327	4.704	4.120	3.286	3.095	-	6.582	4.4901
Asy	0.042	2.046	2.231	3.498	0.847	1.364	1.530	2.602	-	0.175	1.592778
Incline walking											
# of strides	*8*	*9*	*11*	*10*	*7*	*7*	*7*	*8*	*7*	*7*	
											Average
Mean	59.836	49.133	57.166	59.836	48.602	64.125	62.099	70.640	59.731	62.900	59.406
Var	10.415	7.021	5.374	10.415	4.888	4.113	4.930	4.594	-	8.282	6.350
Asy	1.171	4.475	1.827	1.171	6.915	11.023	7.492	7.587	-	13.710	6.152
Rock surface											
# of strides	*6*	*6*	*8*	*3*	*6*	*6*	*5*	*4*	*8*	*7*	
											Average
Mean	65.381	56.778	54.643	65.381	52.102	69.335	62.986	70.574	70.731	67.267	63.517
Var	2.134	6.673	3.368	2.134	4.897	4.121	4.620	1.863	-	4.436	3.860
Asy	9.657	16.532	0.359	9.657	5.990	3.727	17.224	0.696	-	19.321	9.240
Stair ascent											
											Average
Mean	34.650	44.121	41.995	34.650	24.666	49.320	43.474	51.407	54.717	48.013	42.701
Var	3.264	2.369	3.942	3.264	-	4.754	3.781	2.653	-	2.491	2.989
Asy	2.901	5.516	0.337	2.901	-	0.463	7.679	4.591	-	4.758	3.643
Stair descent											
											Average
Mean	75.746	73.257	67.150	75.746	58.536	77.045	71.726	82.048	71.591	80.478	73.332
Var	8.708	7.392	3.906	8.708	-	5.847	6.227	5.500	-	7.141	6.928
Asy	0.841	1.540	4.590	0.841	-	5.807	4.293	5.964	-	1.896	3.221

(-) parameter not available due to data collection or synchronisation error

Table C2 Kinematic knee joint angles (degree) of SS

Stroke Survivors								
	Indoor level walking				***Outdoor level walking***			
	1	**2**	**3** ^{np}		**1**	**2**	**3** ^{np}	
# of strides	*80*	*110*	*91*		*95*	*125*	*108*	
				Average				**Average**
Mean	46.786	49.687	47.888	48.12033	50.782	53.251	52.255	52.096
Var	5.511	5.887	-	6.063667	4.682	6.002	-	5.297
Asy	17.746	26.757	-	22.2515	13.099	26.740	-	19.9195
	Stair ascent				***Stair descent***			
	1	**2**	**3** ^{np}		**1**	**2**	**3** ^{np}	
				Average				**Average**
Mean	32.485	40.762	36.096	36.44767	56.780	74.891	60.844	64.171
Var	5.108	5.868	-	4.712	8.003	6.999	-	7.262
Asy	14.952	2.103	-	8.5275	8.452	2.886	-	5.669

(-) parameter not available due to data collection or synchronisation error,
(np) non paretic side only due to failing to detect IC-FC times

D. EMG, burst timing and durations during stair ambulation

EMG, burst timing and durations (HP): The muscle activation patterns during stair ascent and descent for both groups were shown in Figure S2. Although muscle burst timing and durations slightly varied from person to person, common muscle activation patterns were revealed during stair ambulation. Findings of EMG muscle activation patterns in our participants are consistent with previous stair ambulation based EMG studies [43, 85].

In stair ascent experiments, TA found active mostly from late stance through swing phase to provide adequate foot clearance. TA muscle activation also found early stance phase in most HP. The activation at the stance phase was related to control of foot inversion-eversion, related to balance control during single limb support [43]. GS muscle bursts were detected in the stance phase (mostly mid-stance) for a short period similar to ground level walking. This finding shows good agreement with [85]. However, contradicts with [43], where GS reported being active during most stance phase. Prevalence of RF bursts was also observed in the stance phase, from early stance to midstance. BF muscle activation observed in both stance and swing phase, mostly around FC point and related to flexion of the knee for the next step over.

In stair descent experiments, TA muscle bursts were detected mostly at the initial stance phase, unlike stair ascent. This activation is potentially related to controlling foot inversion-eversion [43]. In some, TA also found active around at initial swing (FCs moments), help sustaining the foot while landing on a surface. GS muscle onset pattern observed around IC moment and lasts until stance to swing transition time. RF muscle activation were observed at the initial stance, IC moments. BF muscle burst found mostly in the opposite phase of RF. Muscle onset of BF at late stance is related to the preparation of limb loading [43].

EMG, burst timing and durations (SS): The common EMG pattern of burst timing and durations observed in HP also observed in SS group, as shown in Figure S1- (d3-d6). Although there are differences in terms of burst timing and durations, it may not be possible to relate these differences with SS group as a result of this pilot study. Because earlier EMG based studies reported that there are other crucial parameters, such as walking velocity and age that affects muscle burst timing and durations [83]. Additionally, the number of studies for muscle activation of SS during stair ambulation is very limited, unlike level walking. Thus, future works will investigate the muscle pattern of SS during stair ambulation with a larger cohort.

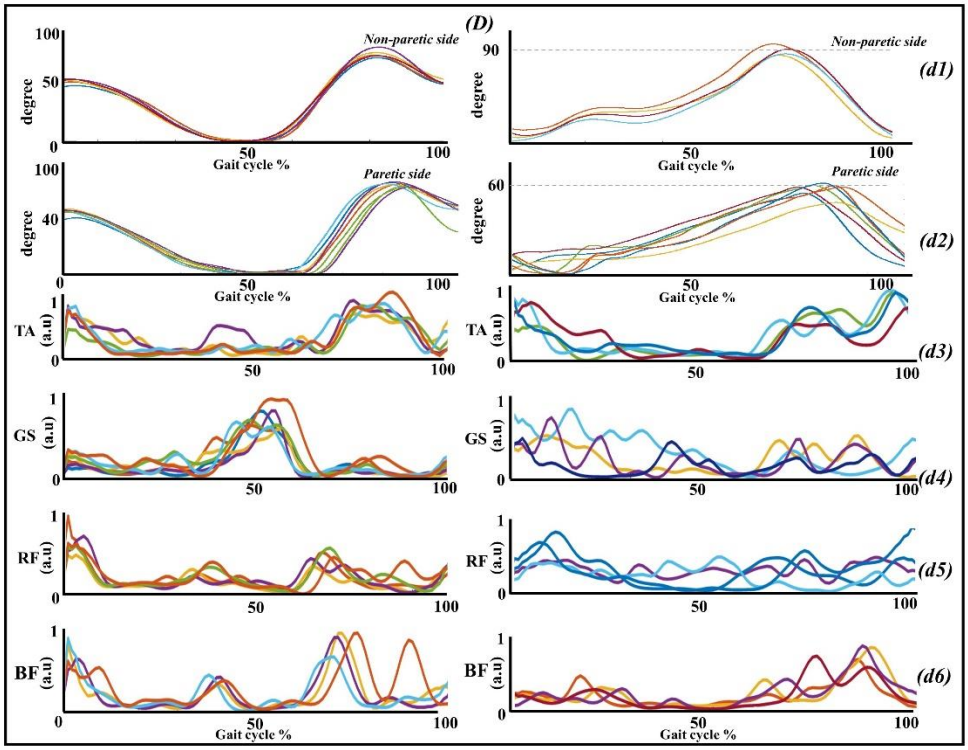

Figure D1. Stroke Gait. (D) stair ascent & descent extracted parameters from the proposed tool. (d1) left panel represents non paretic side knee flexion during stair ascent and right panel represent paretic side knee flexion during stair descent. (d2) left panel represents paretic side knee flexion during stair ascent and right panel represent non paretic side knee flexion during stair descent. Left panel of (d3-d6) presents typical lower limb muscle activations during stair ascent. Right panel of (d3-d6) presents typical lower limb muscle activations during stair descent. a.u, Arbitrary unit-peak normalised EMG

Table D1 Spatio-temporal gait characteristics of SS ground level walking in indoor and outdoor for the right and left sides. SS (#3) paretic, non-paretic data is not presented due to failing to detect paretic side IC-FC moments.

	Indoor						***Outdoor***					
	Np			***P***			***Np***			***P***		
	1	***2***		***1***	***2***		***1***	***2***		***1***	***2***	
RHYTHM			***Average***			***Average***			***Average***			***Average***
Mean Step T.ime (s)	0.558	0.57	0.564	0.754	0.575	**0.6645**	0.465	0.648	0.5565	0.63	0.606	**0.618**
Mean Stance Time (s)	0.83	0.673	**0.7515**	0.701	0.66	0.6805	0.736	0.427	**0.5815**	0.602	0.459	0.5305
Mean Swing Time (s)	0.48	0.467	0.4735	0.603	0.486	**0.5445**	0.425	0.503	0.464	0.528	0.545	**0.5365**
VARIABILITY												
Step Time Var (s)	0.004	0.004	**0.004**	0.003	0.002	0.0025	0.007	0.007	**0.007**	0.002	0.005	0.0035
Stance Time Var (s)	0.003	0.001	0.002	0.004	0.004	**0.004**	0.001	0.001	0.001	0.001	0.001	0.001
Swing Time Var (s)	0.004	0.004	**0.004**	0.003	0.003	0.003	0.001	0.001	0.001	0.001	0.001	0.001
Mean K.F.E angle(°)	55.659	63.065	**59.362**	37.913	36.308	37.1105	57.164	63.237	**60.2005**	42.576	38.311	40.4435

(K.F.E) knee flexion angle (degree), Np=non paretic side, P=paretic side
Bold indicate greater mean values comparing non paretic side to paretic side

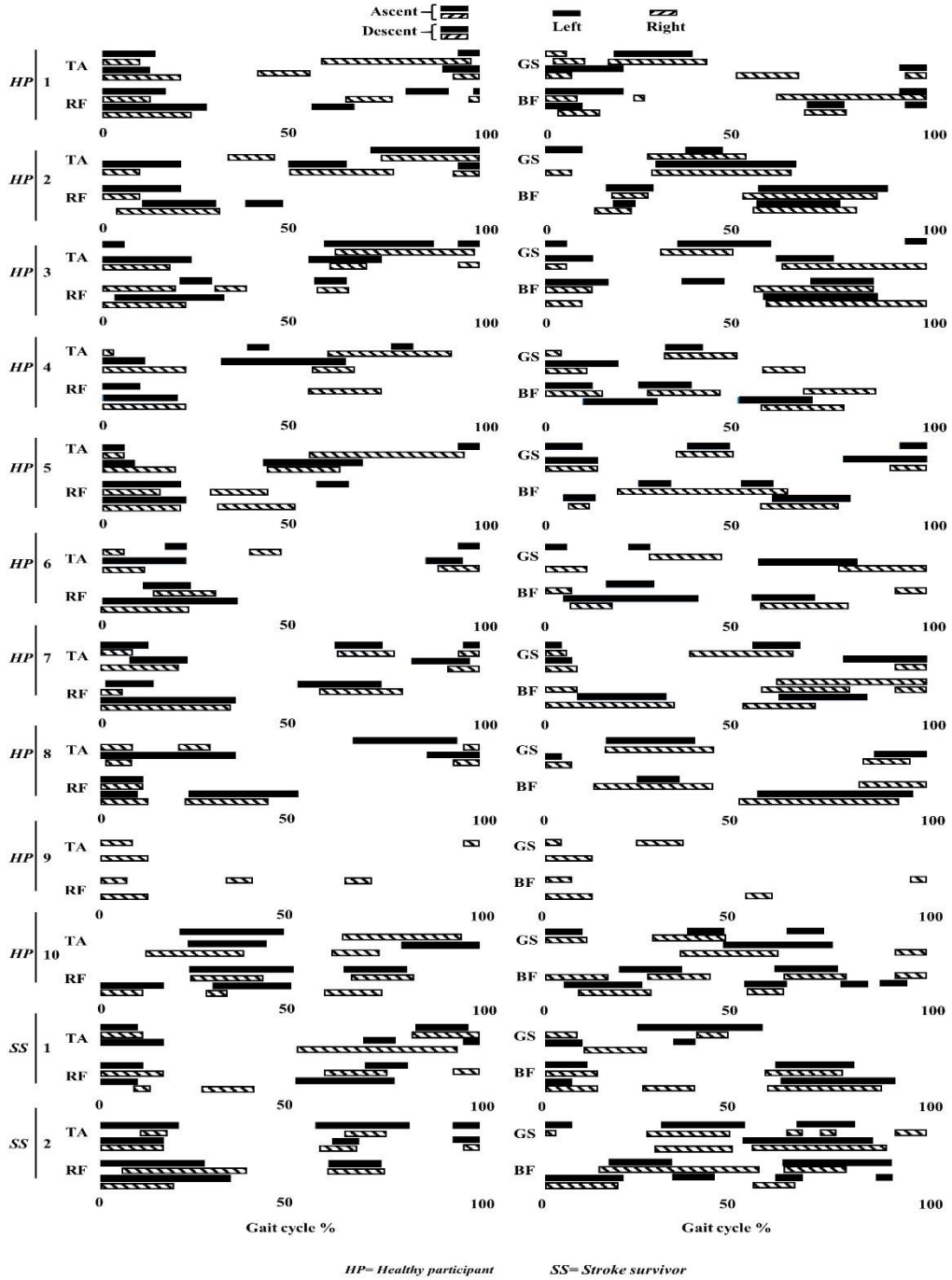

Figure D2. Muscle activity pattern for stair ambulation, healthy participants and stroke survivors